LONESTAR: Analog Beamforming Codebooks for Full-Duplex Millimeter Wave Systems

Ian P. Roberts, *Graduate Student Member, IEEE,* Sriram Vishwanath, *Fellow, IEEE,* and Jeffrey G. Andrews, *Fellow, IEEE*

***Abstract*—This work develops LONESTAR, a novel enabler of full-duplex millimeter wave (mmWave) communication systems through the design of analog beamforming codebooks. LONESTAR codebooks deliver high beamforming gain and broad coverage while simultaneously reducing the self-interference coupled by transmit and receive beams at a full-duplex mmWave transceiver. Our design framework accomplishes this by tolerating some variability in transmit and receive beamforming gain to strategically shape beams that reject self-interference spatially while accounting for digitally-controlled analog beamforming networks and self-interference channel estimation error. By leveraging the coherence time of the self-interference channel, a mmWave system can use the same LONESTAR design over many time slots to serve several downlink-uplink user pairs in a full-duplex fashion without the need for additional self-interference cancellation. Compared to those using conventional codebooks, full-duplex mmWave systems employing LONESTAR codebooks can mitigate higher levels of self-interference, tolerate more cross-link interference, and demand lower SNRs in order to outperform half-duplex operation—all while supporting beam alignment. This makes LONESTAR a potential standalone solution for enabling simultaneous transmission and reception in mmWave systems, from which it derives its name.**

***Index Terms*—Full-duplex, millimeter wave, phased arrays, beamforming, self-interference, codebooks, beam alignment.**

I. INTRODUCTION

CODEBOOK-BASED analog beamforming is a critical component of millimeter wave (mmWave) communication systems [2], [3]. Rather than estimate a high-dimensional multiple-input multiple-output (MIMO) channel and subsequently configure an analog beamforming network, modern mmWave systems instead rely on beam alignment procedures to identify promising beamforming directions, typically via exploration of a codebook of candidate beams [2]–[4]. This offers a simple and robust way to configure an analog beamforming network without downlink/uplink MIMO channel knowledge *a priori*, which is expensive to obtain in practice. In conventional half-duplex mmWave systems, it is relatively straightforward to design a beamforming codebook that delivers coverage over a desired region [4]. For instance, conjugate beamforming and discrete Fourier transform (DFT) beamforming are simple ways to construct a set of beams that steer high gain in specific directions using digitally-controlled phase shifters [5]. Other codebook designs make use of amplitude control via digitally-controlled attenuators or variable-gain amplifiers (VGAs) to shape beams with suppressed side lobes in an effort to reduce interference [6]–[8].

The design of beamforming codebooks for in-band full-duplex mmWave communication systems, on the other hand, is not so straightforward. A full-duplex mmWave transceiver with separate transmit and receive arrays, for instance, will juggle a transmit beam and a receive beam at the same time over the same frequency spectrum, potentially serving two different half-duplex users. These transmit and receive beams couple over the MIMO channel that manifests between the arrays, plaguing a desired receive signal with self-interference. In a recent measurement campaign [9], we observed that the degree of this self-interference is typically prohibitively high for full-duplex operation in practical mmWave systems. This, along with the fact that modern mmWave systems rely on codebook-based beam alignment, motivates the need for beamforming codebooks designed specifically for full-duplex mmWave systems—as opposed to using conventional codebooks made for half-duplex systems [10]. In this work, we present LONESTAR, the first framework for designing beamforming codebooks for full-duplex mmWave communication systems. LONESTAR produces transmit and receive codebooks that deliver high beamforming gain and provide broad coverage to downlink and uplink users while coupling low self-interference between the transmit and receive beams of a full-duplex transceiver. By supporting beam alignment and reducing self-interference to levels near or below the noise floor regardless of which transmit and receive beams are selected from its codebooks, LONESTAR can serve as a potential standalone solution for simultaneous transmission and reception, from which it derives its name.

Rather than using analog and digital self-interference cancellation to enable full-duplex as was commonly done in sub-6 GHz systems [11], recent work has proposed solely using beamforming to mitigate self-interference in mmWave communication systems [10], [12]–[24]. Such methods largely aim to take advantage of the high-dimensional spatial domain afforded by dense mmWave antenna arrays to tackle self-interference via strategic design of transmit and receive beamformers. However, there are key practical hurdles neglected by existing designs that we address in this work holistically.

Manuscript received June 22, 2022; revised October 17, 2022; accepted December 27, 2022. The work of Ian P. Roberts was supported by the National Science Foundation Graduate Research Fellowship Program under Grant DGE-1610403. Corresponding author: Ian P. Roberts (ipr@utexas.edu).

The authors are with 6G@UT in the Wireless Networking and Communications Group at the University of Texas at Austin, Austin, TX 78712, USA.

This work is an extension of [1].

Some designs [12]–[21] have neglected codebook-based analog beamforming, assuming the ability to fine-tune each phase shifter in real-time, and do not account for digitally-controlled phase shifters of practical analog beamforming networks. Most designs have assumed a lack of amplitude control, even though it is not uncommon to have both digitally-controlled phase shifters and attenuators or VGAs in practice [25]–[27]. In addition, existing solutions [12]–[18] have assumed real-time knowledge of the downlink and uplink MIMO channels—along with that of the self-interference MIMO channel—to configure transmit and receive beams. As such, they neglect beam alignment and rely on frequent estimation of high-dimensional MIMO channels, both of which are practical shortcomings. Furthermore, the majority of existing designs are for hybrid digital/analog beamforming architectures and are not necessarily suitable for analog-only beamforming systems, which are common in practice for power and cost efficiency.

To our knowledge, the only existing beamforming-based full-duplex solution suitable for analog beamforming mmWave systems that supports codebook-based beam alignment is our recent work called STEER [24]. The work herein and that of STEER tackle a very similar problem but their approaches differ significantly due to differences in the assumption of self-interference channel knowledge. In STEER, we relied on measurements of candidate beam pairs to strategically select transmit and receive beams that couple low self-interference while maintaining high gain in desired directions. In this work, rather than use measurements of self-interference, we instead rely on (imperfect) estimation of the self-interference MIMO channel, which LONESTAR uses to construct transmit and receive codebooks such that every transmit-receive beam pair couples low self-interference. STEER was validated using an actual 28 GHz phased array platform and proved to be a promising full-duplex solution, but it remains unclear if STEER's success will translate to other platforms. Presented herein, LONESTAR is more flexible to the particular self-interference channel than STEER since it makes use of more degrees of freedom, meaning it has the potential to better generalize across mmWave platforms.

LONESTAR: Beamforming codebooks for full-duplex mmWave systems. In this work, we present LONESTAR, a novel approach to enable full-duplex mmWave systems through the use of analog beamforming codebooks strategically designed to reduce self-interference and simultaneously deliver high beamforming gain. We present an optimization framework for designing transmit and receive codebooks that minimize the self-interference coupled between all transmit-receive beam pairs while constraining the coverage they provide over defined service regions. A full-duplex mmWave transceiver can independently select any transmit beam and any receive beam from LONESTAR codebooks and, with reasonable confidence, can expect low self-interference. LONESTAR codebooks are designed at the full-duplex transceiver following estimation of the self-interference MIMO channel (which need not be perfect), do not require downlink/uplink MIMO channel knowledge, and do not demand any over-the-air feedback to/from users. After their construction, LONESTAR codebooks can be used to conduct beam alignment and serve any downlink-uplink user pair in a full-duplex fashion thereafter with reduced self-interference. Importantly, LONESTAR accounts for limited phase and amplitude control present in practical analog beamforming networks.

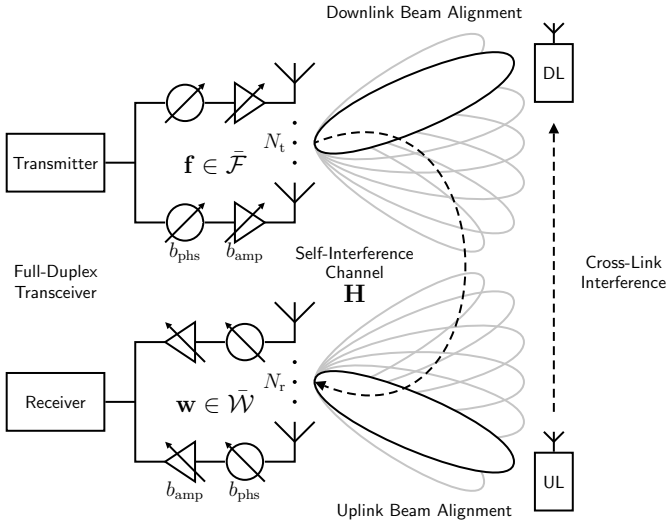

Fig. 1. A full-duplex mmWave BS transmits to a downlink user while receiving from an uplink user in-band. In doing so, self-interference couples between its transmit beam $\mathbf{f}$ and receive beam $\mathbf{w}$ across the channel $\mathbf{H}$, and cross-link interference is inflicted on the downlink user by the uplink user. Transmit and receive beams are selected from codebooks $\bar{\mathcal{F}}$ and $\bar{\mathcal{W}}$ via beam alignment. In this work, we design these codebooks such that any selected $\mathbf{f} \in \bar{\mathcal{F}}$ and $\mathbf{w} \in \bar{\mathcal{W}}$ will couple low self-interference.

Validation of LONESTAR as a full-duplex solution. We use extensive simulation to evaluate LONESTAR, which highlights its potential to enable full-duplex operation in mmWave systems without any additional self-interference cancellation. We compare full-duplex performance with LONESTAR codebooks against that with conventional codebooks to illustrate that LONESTAR can supply an additional 10–50 dB of robustness to self-interference, depending on hardware constraints, without sacrificing high beamforming gain. This translates to impressive spectral efficiency gains that, with high-resolution phase shifters and attenuators, can approach the interference-free capacity of conventional codebooks. Simulation further illustrates LONESTAR's robustness to self-interference channel estimation error and to cross-link interference between downlink and uplink users. Our results motivate a variety of future work including self-interference channel modeling and reliable self-interference channel estimation.

II. SYSTEM MODEL

Illustrated in Fig. 1, we consider a mmWave BS that employs separate, independently-controlled antenna arrays for transmission and reception that are used to serve a downlink user and uplink user in a full-duplex fashion (simultaneously and in-band). Note that these users may come from different distributions, depending on the array configuration (e.g., consider a sectorized BS). One may imagine full-duplex integrated access and backhaul (IAB), for instance, as an attractive

application of this work in mmWave networks [28]–[32]. Let N_{t} and N_{r} be the number of transmit and receive antennas, respectively, at the arrays of the full-duplex BS. We denote as $\mathbf{a}_{\mathrm{tx}}(\theta) \in \mathbb{C}^{N_{\mathrm{t}}\times 1}$ and $\mathbf{a}_{\mathrm{rx}}(\theta) \in \mathbb{C}^{N_{\mathrm{r}}\times 1}$ its transmit and receive array response vectors, respectively, in the direction θ. These array response vectors for any θ can be computed based on the BS array geometries [5], [33], and we follow the convention $\|\mathbf{a}_{\mathrm{tx}}(\theta)\|_2^2 = N_{\mathrm{t}}$ and $\|\mathbf{a}_{\mathrm{rx}}(\theta)\|_2^2 = N_{\mathrm{r}}$. To simplify presentation, users are single-antenna devices, but this is not a necessary assumption.

We consider an analog beamforming system at the BS, though the codebook design herein could also be used by hybrid beamforming systems and even generalized to digital beamforming. Let $\mathbf{f} \in \mathbb{C}^{N_{\mathrm{t}}\times 1}$ be the beamforming vector used at the transmitter of the BS and $\mathbf{w} \in \mathbb{C}^{N_{\mathrm{r}}\times 1}$ be the beamforming vector used at its receiver. We consider analog beamforming networks equipped with phase shifters and attenuators which are digitally controlled with b_{phs} and b_{amp} bits, respectively.[1] Each beamforming weight must not exceed unit magnitude, understood by the fact that attenuators are used for amplitude control.

$$|[\mathbf{f}]_m| \leq 1 \;\forall\; m = 1, \ldots, N_{\mathrm{t}} \tag{1}$$

$$|[\mathbf{w}]_n| \leq 1 \;\forall\; n = 1, \ldots, N_{\mathrm{r}} \tag{2}$$

Directly from (1) and (2), we have $\|\mathbf{f}\|_2^2 \leq N_{\mathrm{t}}$ and $\|\mathbf{w}\|_2^2 \leq N_{\mathrm{r}}$. Capturing limited phase and amplitude control, let $\mathcal{F} \subset \mathbb{C}^{N_{\mathrm{t}}\times 1}$ and $\mathcal{W} \subset \mathbb{C}^{N_{\mathrm{r}}\times 1}$ be the sets of all possible physically realizable beamforming vectors $\mathbf{f}$ and $\mathbf{w}$, respectively; hence, it is practically required that $\mathbf{f} \in \mathcal{F}$ and $\mathbf{w} \in \mathcal{W}$. We assume the BS and uplink user transmit with powers $P_{\mathrm{tx}}^{\mathrm{BS}}$ and $P_{\mathrm{tx}}^{\mathrm{UE}}$, respectively. Additive noise powers per antenna at the BS and downlink user are respectively $P_{\mathrm{noise}}^{\mathrm{BS}}$ and $P_{\mathrm{noise}}^{\mathrm{UE}}$.

Taking the perspective of the full-duplex BS, let $\mathbf{h}_{\mathrm{tx}}^* \in \mathbb{C}^{1\times N_{\mathrm{t}}}$ be the transmit channel vector from the BS to the downlink user. Let $\mathbf{h}_{\mathrm{rx}} \in \mathbb{C}^{N_{\mathrm{r}}\times 1}$ be the receive channel from the uplink user to the BS. We normalize each of these channels such that $\|\mathbf{h}_{\mathrm{tx}}\|_2^2 = N_{\mathrm{t}}$ and $\|\mathbf{h}_{\mathrm{rx}}\|_2^2 = N_{\mathrm{r}}$ and abstract out their large-scale gains as inverse path losses G_{tx}^2 and G_{rx}^2, respectively. Since transmission and reception happen simultaneously and in-band, a self-interference channel $\mathbf{H} \in \mathbb{C}^{N_{\mathrm{r}}\times N_{\mathrm{t}}}$ manifests between the transmit and receive arrays of the full-duplex BS. Currently, there is not a reliable, measurement-backed model for the self-interference channel $\mathbf{H}$ [9], [10]. As such, the design herein is not based on any assumption of $\mathbf{H}$, and we evaluate our design using multiple channel models in Section VII. To abstract out the large-scale gain of the self-interference channel from its spatial characteristics, we impose $\|\mathbf{H}\|_{\mathrm{F}}^2 = N_{\mathrm{t}} \cdot N_{\mathrm{r}}$ and let G^2 be its inverse path loss based on the inherent isolation between the arrays (practically, $G^2 \ll 0$ dB). With the downlink and uplink users operating simultaneously and in-band, a scalar cross-link interference channel h_{CL} arises between them. We normalize $|h_{\mathrm{CL}}|^2 = 1$ and let G_{CL}^2 be the inverse path loss of the cross-link interference channel, which practically depends on the users' locations and the environment.

[1]Existing mmWave literature often considers networks with only phase shifters, but it is not uncommon for practical mmWave arrays to also be equipped with attenuators or VGAs for amplitude control [25]–[27]. Our formulation could also capture beamforming networks employing VGAs (rather than attenuators) by including their maximum gain settings in (1) and (2), for instance.

III. Problem Formulation and Motivation

Using the established system model, we now further formulate and motivate this work. Again taking the perspective of the full-duplex BS, we refer to downlink as the *transmit link* and to uplink as the *receive link*. The signal-to-interference-plus-noise ratios (SINRs) of these links can be expressed as

$$\mathsf{SINR}_{\mathrm{tx}} = \frac{\mathsf{SNR}_{\mathrm{tx}}}{1 + \mathsf{INR}_{\mathrm{tx}}}, \qquad \mathsf{SINR}_{\mathrm{rx}} = \frac{\mathsf{SNR}_{\mathrm{rx}}}{1 + \mathsf{INR}_{\mathrm{rx}}}, \tag{3}$$

each of which being dictated by its respective signal-to-noise ratio (SNR) and interference-to-noise ratio (INR). For some transmit and receive beams $\mathbf{f}$ and $\mathbf{w}$, the SNRs of the transmit and receive links are respectively

$$\mathsf{SNR}_{\mathrm{tx}} = \frac{P_{\mathrm{tx}}^{\mathrm{BS}} \cdot G_{\mathrm{tx}}^2 \cdot |\mathbf{h}_{\mathrm{tx}}^* \mathbf{f}|^2}{N_{\mathrm{t}} \cdot P_{\mathrm{noise}}^{\mathrm{UE}}}, \tag{4}$$

$$\mathsf{SNR}_{\mathrm{rx}} = \frac{P_{\mathrm{tx}}^{\mathrm{UE}} \cdot G_{\mathrm{rx}}^2 \cdot |\mathbf{w}^* \mathbf{h}_{\mathrm{rx}}|^2}{\|\mathbf{w}\|_2^2 \cdot P_{\mathrm{noise}}^{\mathrm{BS}}}, \tag{5}$$

where dividing by N_{t} in (4) handles power splitting within the transmit array and by $\|\mathbf{w}\|_2^2$ in (5) handles noise combining at the receive array. By virtue of the fact that $N^2 = \|\mathbf{h}\|_2^2 \cdot \|\mathbf{x}\|_2^2 = \max_{\mathbf{x}} |\mathbf{h}^*\mathbf{x}|^2$ s.t. $\|\mathbf{x}\|_2^2 \leq N, \|\mathbf{h}\|_2^2 = N$, the maximum SNRs are denoted with an overline as

$$\overline{\mathsf{SNR}}_{\mathrm{tx}} = \frac{P_{\mathrm{tx}}^{\mathrm{BS}} \cdot G_{\mathrm{tx}}^2 \cdot N_{\mathrm{t}}}{P_{\mathrm{noise}}^{\mathrm{UE}}} \geq \mathsf{SNR}_{\mathrm{tx}}, \tag{6}$$

$$\overline{\mathsf{SNR}}_{\mathrm{rx}} = \frac{P_{\mathrm{tx}}^{\mathrm{UE}} \cdot G_{\mathrm{rx}}^2 \cdot N_{\mathrm{r}}}{P_{\mathrm{noise}}^{\mathrm{BS}}} \geq \mathsf{SNR}_{\mathrm{rx}}. \tag{7}$$

In other words, these are achieved only when users are delivered maximum beamforming gain.

When juggling a transmit beam $\mathbf{f}$ and receive beam $\mathbf{w}$ in a full-duplex fashion, the BS couples self-interference, leading to a receive link INR of

$$\mathsf{INR}_{\mathrm{rx}} = \frac{P_{\mathrm{tx}}^{\mathrm{BS}} \cdot G^2 \cdot |\mathbf{w}^* \mathbf{H} \mathbf{f}|^2}{N_{\mathrm{t}} \cdot \|\mathbf{w}\|_2^2 \cdot P_{\mathrm{noise}}^{\mathrm{BS}}}, \tag{8}$$

where $|\mathbf{w}^*\mathbf{H}\mathbf{f}|^2$ captures the transmit and receive beam coupling over the self-interference channel. Strategically designing $\mathbf{f}$ and $\mathbf{w}$ according to $\mathbf{H}$ can therefore reduce self-interference. Based on our normalizations, the worst-case coupling between transmit and receive beams at the full-duplex BS is $N_{\mathrm{t}}^2 \cdot N_{\mathrm{r}}^2 = \max |\mathbf{w}^*\mathbf{H}\mathbf{f}|^2$, leading to a maximum possible $\mathsf{INR}_{\mathrm{rx}}$ of

$$\overline{\mathsf{INR}}_{\mathrm{rx}} = \frac{P_{\mathrm{tx}}^{\mathrm{BS}} \cdot G^2 \cdot N_{\mathrm{t}} \cdot N_{\mathrm{r}}}{P_{\mathrm{noise}}^{\mathrm{BS}}} \geq \mathsf{INR}_{\mathrm{rx}}, \tag{9}$$

which we use as a metric to capture the inherent strength of self-interference at the BS. Note that $\overline{\mathsf{INR}}_{\mathrm{rx}}$ depends solely on system parameters and artifacts at the BS. We denote as $\mathsf{INR}_{\mathrm{tx}}$ the INR incurred at the downlink user due to cross-link interference.

$$\mathsf{INR}_{\mathrm{tx}} = \frac{P_{\mathrm{tx}}^{\mathrm{UE}} \cdot G_{\mathrm{CL}}^2 \cdot |h_{\mathrm{CL}}|^2}{P_{\mathrm{noise}}^{\mathrm{UE}}} \tag{10}$$

Note that cross-link interference $\mathsf{INR}_{\rm tx}$ only depends on its inherent channel and path loss, not on $\mathbf{f}$ nor $\mathbf{w}$. In this work, we do not consider uplink power control as a means to reduce cross-link interference, though this could be useful in practice.

The achievable spectral efficiencies on each link, treating interference as noise, are

$$R_{\rm tx} = \log_2(1+\mathsf{SINR}_{\rm tx}), \quad R_{\rm rx} = \log_2(1+\mathsf{SINR}_{\rm rx}), \quad (11)$$

whereas the capacities of the two links are $C_{\rm tx} = \log_2\big(1+\overline{\mathsf{SNR}}_{\rm tx}\big)$ and $C_{\rm rx} = \log_2\big(1+\overline{\mathsf{SNR}}_{\rm rx}\big)$. We assume no forms of active self-interference cancellation are employed at the BS. Instead, we will rely solely on beamforming to mitigate self-interference and enable full-duplex operation. The degree of self-interference coupled at the full-duplex BS in (8) depends on the transmit beam $\mathbf{f}$ and receive beam $\mathbf{w}$, each of which also dictates its respective link's SNR. As such, it is important that $\mathbf{f}$ and $\mathbf{w}$ couple low self-interference and deliver high $\mathsf{SNR}_{\rm tx}$ and $\mathsf{SNR}_{\rm rx}$ in an effort to achieve high sum spectral efficiency $R_{\rm tx}+R_{\rm rx}$.

In this work, we rely on estimation of the self-interference MIMO channel $\mathbf{H}$ at the full-duplex BS, but do not assume any knowledge of the downlink or uplink channels $\mathbf{h}_{\rm tx}$ and $\mathbf{h}_{\rm rx}$. We do not assume perfect estimation of $\mathbf{H}$ but rather model its imperfections as

$$\mathbf{H} = \bar{\mathbf{H}} + \mathbf{\Delta}, \qquad [\mathbf{\Delta}]_{i,j} \sim \mathcal{N}_{\mathbb{C}}\big(0,\epsilon^2\big) \;\forall\; i,j, \qquad (12)$$

where $\bar{\mathbf{H}}$ is the estimate of $\mathbf{H}$ and $\mathbf{\Delta}$ captures independently and identically distributed (i.i.d.) Gaussian estimation error with mean 0 and variance ϵ^2. Self-interference channel estimation in full-duplex mmWave systems is an open research problem [10]. As such, the choice of a particular estimation error model is currently difficult to practically justify, but we remark that other error models (e.g., norm-based models) may be encompassed by our Gaussian model with arbitrarily high probability for appropriately chosen ϵ^2.

It is our hope that $\mathbf{H}$ can be estimated with high fidelity for three reasons. First, the self-interference channel is likely much stronger than traditional downlink/uplink MIMO channels, meaning it may be estimated with higher accuracy. Second, the estimation of $\mathbf{H}$ takes place across the arrays of the BS, meaning it does not consume resources for feedback and does not suffer from feedback quantization. Third, we expect that the self-interference channel will be fairly static on the timescale of data transmissions, especially the portion caused by direct coupling between the arrays[2], which will presumably dominate. Together, all of this suggests that the estimation of $\mathbf{H}$ may be more thorough and precise than that of traditional downlink/uplink MIMO channels. Nonetheless, our design in the next section incorporates channel estimation error. In our numerical evaluation in Sections VI–VII, one self-interference channel model we consider is the spherical-wave model, which has been widely used in the related literature to capture near-field propagation between the transmit and receive arrays. Recent work [34] has presented a scheme for efficiently and accurately estimating such channels, especially considering the presumably high strength of self-interference $\overline{\mathsf{INR}}_{\rm rx}$. Self-interference channel estimation and its coherence time would be valuable directions for future work, especially in practical systems. The key practical advantages of LoneSTAR rely on the self-interference channel being sufficiently static over many downlink/uplink time slots, which we assume herein.

[2]In [9], we observed that 28 GHz self-interference in an anechoic chamber was nearly static on the order of minutes, at least.

IV. Beamforming Codebook Design for Full-Duplex mmWave Systems

Practical mmWave systems—which have operated in a half-duplex fashion thus far—rely on beam alignment to identify beams that deliver high beamforming gain when serving a particular user. This is typically done by sweeping a set of candidate beams called a *codebook* and measuring the reference signal received power (RSRP) for each beam candidate in order to select which is used to close a link. This procedure allows a mmWave system to reliably deliver high beamforming gain without the need for downlink/uplink MIMO channel knowledge, which is expensive to obtain in practice.

As mentioned in the introduction, plenty of existing work has designed particular transmit and receive beams $\mathbf{f}$ and $\mathbf{w}$ to use at the BS to reduce self-interference when full-duplexing downlink and uplink users, but most existing designs have a number of practical shortcomings. In this work, we instead design transmit and receive beam codebooks $\bar{\mathcal{F}}$ and $\bar{\mathcal{W}}$, from which the BS can draw for $\mathbf{f}$ and $\mathbf{w}$ following conventional beam alignment. Note that $\bar{\mathcal{F}}$ and $\bar{\mathcal{W}}$ are not necessarily used directly for beam alignment but rather could be drawn from following whatever beam alignment procedure is performed. The goal of our design—which we call LoneSTAR—is to create codebooks that a full-duplex mmWave BS can use to deliver high beamforming gain to users while simultaneously mitigating self-interference. This will be achieved by strategically designing $\bar{\mathcal{F}}$ and $\bar{\mathcal{W}}$ such that their transmit and receive beams couple low self-interference, regardless of which $\mathbf{f} \in \bar{\mathcal{F}}$ and $\mathbf{w} \in \bar{\mathcal{W}}$ are selected following beam alignment. In contrast, codebooks created for conventional mmWave systems can deliver high beamforming gain but are not necessarily robust to self-interference if used in full-duplex systems [10]. In fact, this was confirmed in our recent measurement campaign [9] and in our recent work [24], both of which showed that conventional beams typically couple prohibitively high amounts of self-interference if used in a practical full-duplex mmWave system.

Our envisioned use of LoneSTAR is depicted in Fig. 2, which illustrates that our codebook design need only be executed once per coherence time of $\mathbf{H}$, allowing the same full-duplex solution to be used over many downlink-uplink user pairs (i.e., data transmissions). This is a key practical advantage of LoneSTAR versus most existing mmWave full-duplex solutions, which we depict in Fig. 3. Most often, existing designs tailor their solutions uniquely for each downlink-uplink user pair and warrant estimation of the downlink and uplink MIMO channels, which itself is impractical in today's systems. On the other hand, a single LoneSTAR design can serve a sequence of downlink-uplink user pairs in a full-duplex fashion without any additional overhead. Moreover, existing

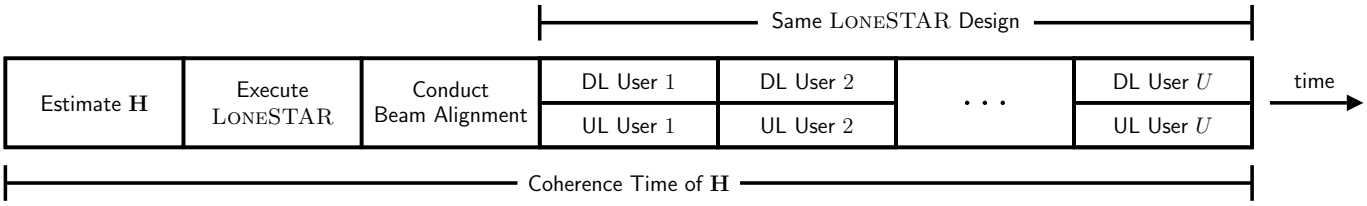

Fig. 2. Following estimation of the self-interference channel $\mathbf{H}$, transmit and receive beam codebooks designed with LONESTAR can be used for beam alignment and subsequently to serve any downlink and uplink users in a full-duplex fashion.

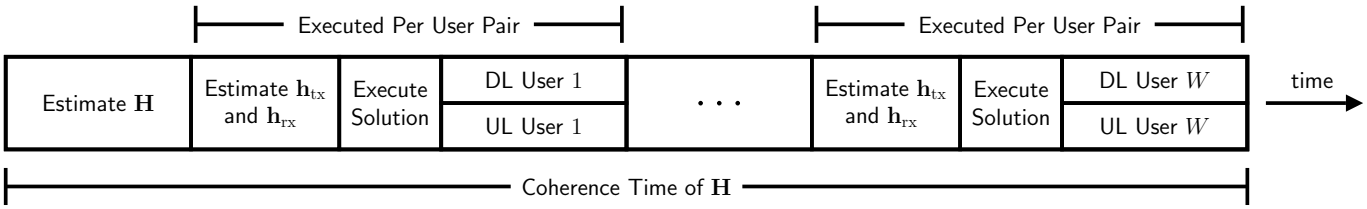

Fig. 3. Most existing beamforming-based full-duplex mmWave solutions require estimation of the downlink and uplink channels and execution of their design for each user pair, leading to a total overhead that scales with the number of users served.

designs typically introduce over-the-air feedback to and from users, whereas LONESTAR does not require this—its design taking place completely at the full-duplex transceiver. Naturally, the coherence time of mmWave self-interference, which is not currently well understood, will be an important factor in justifying the use of LONESTAR since it dictates how frequently $\mathbf{H}$ must be estimated and how often LONESTAR needs to be re-executed. It should be noted, however, that existing designs also rely on estimation of the self-interference channel, meaning they too are subjected to its coherence time. If our design sufficiently mitigates self-interference between all beam pairs, a mmWave BS employing LONESTAR codebooks can seamlessly operate in a full-duplex fashion without any additional self-interference cancellation—any transmit and receive beams selected via beam alignment will couple low self-interference.

A. Quantifying Our Codebook Design Criteria

In pursuit of transmit and receive beam codebooks that reliably offer high sum spectral efficiency $R_{\text{tx}}+R_{\text{rx}}$, we desire sets of transmit and receive beams that can deliver high SNR_{tx} and SNR_{rx} while coupling low self-interference INR_{rx}. As mentioned, cross-link interference INR_{tx} is fixed for a given downlink-uplink user pair since it does not depend on $\mathbf{f}$ nor $\mathbf{w}$. In the remainder of this section, we first quantify our codebook design criteria and then assemble a design problem that tackles both objectives jointly. As we proceed with outlining our design, please refer to Fig. 4 for an illustration of the inputs and outputs of LONESTAR.

Definition 1: Transmit and receive coverage regions. Let $\mathcal{A}_{\text{tx}}$ be a set of M_{tx} directions—or a *transmit coverage region*—that our transmit codebook $\bar{\mathcal{F}}$ aims to serve, and let $\mathcal{A}_{\text{rx}}$ be a *receive coverage region* defined analogously.

$$\mathcal{A}_{\text{tx}} = \left\{\theta_{\text{tx}}^{(i)} : i = 1, \ldots, M_{\text{tx}}\right\} \tag{13}$$

$$\mathcal{A}_{\text{rx}} = \left\{\theta_{\text{rx}}^{(j)} : j = 1, \ldots, M_{\text{rx}}\right\} \tag{14}$$

Here, $\theta_{\text{tx}}^{(i)}$ and $\theta_{\text{rx}}^{(j)}$ each may capture azimuthal and elevational components of a given direction.

Definition 2: Transmit and receive beamforming codebooks. We index the M_{tx} beams in $\bar{\mathcal{F}}$ and the M_{rx} beams in $\bar{\mathcal{W}}$ according to $\mathcal{A}_{\text{tx}}$ and $\mathcal{A}_{\text{rx}}$, respectively, as $\bar{\mathcal{F}} = \{\mathbf{f}_1, \ldots, \mathbf{f}_{M_{\text{tx}}}\}$ and $\bar{\mathcal{W}} = \{\mathbf{w}_1, \ldots, \mathbf{w}_{M_{\text{rx}}}\}$, where $\mathbf{f}_i \in \mathcal{F}$ is responsible for transmitting toward $\theta_{\text{tx}}^{(i)}$ and $\mathbf{w}_j \in \mathcal{W}$ is responsible for receiving from $\theta_{\text{rx}}^{(j)}$. Using this notation, we build the transmit codebook matrix $\mathbf{F}$ by stacking transmit beams $\mathbf{f}_i$ as follows and the receive codebook matrix $\mathbf{W}$ analogously.

$$\mathbf{F} = \begin{bmatrix}\mathbf{f}_1 & \mathbf{f}_2 & \cdots & \mathbf{f}_{M_{\text{tx}}}\end{bmatrix} \in \mathbb{C}^{N_{\text{t}} \times M_{\text{tx}}} \tag{15}$$

$$\mathbf{W} = \begin{bmatrix}\mathbf{w}_1 & \mathbf{w}_2 & \cdots & \mathbf{w}_{M_{\text{rx}}}\end{bmatrix} \in \mathbb{C}^{N_{\text{r}} \times M_{\text{rx}}} \tag{16}$$

Definition 3: Transmit and receive beamforming gains. Let $g_{\text{tx}}^2\left(\theta_{\text{tx}}^{(i)}\right)$ be the transmit beamforming gain afforded by $\mathbf{f}_i$ in the direction $\theta_{\text{tx}}^{(i)}$ and $g_{\text{rx}}^2\left(\theta_{\text{rx}}^{(j)}\right)$ be the receive beamforming gain afforded by $\mathbf{w}_j$ in the direction $\theta_{\text{rx}}^{(j)}$, expressed as

$$g_{\text{tx}}^2\left(\theta_{\text{tx}}^{(i)}\right) = \left|\mathbf{a}_{\text{tx}}\left(\theta_{\text{tx}}^{(i)}\right)^* \mathbf{f}_i\right|^2 \leq N_{\text{t}}^2, \tag{17}$$

$$g_{\text{rx}}^2\left(\theta_{\text{rx}}^{(j)}\right) = \left|\mathbf{a}_{\text{rx}}\left(\theta_{\text{rx}}^{(j)}\right)^* \mathbf{w}_j\right|^2 \leq N_{\text{r}}^2. \tag{18}$$

The transmit and receive beamforming gains are upper-bounded by N_{t}^2 and N_{r}^2, respectively, by virtue of normalizations presented in our system model. Maximum beamforming gains can be achieved toward any direction θ with beams $\mathbf{f} = \mathbf{a}_{\text{tx}}(\theta)$ and $\mathbf{w} = \mathbf{a}_{\text{rx}}(\theta)$, respectively, often referred to as *conjugate beamforming* or *matched filter beamforming* [5].

Definition 4: Average self-interference coupled. The coupling between the i-th transmit beam $\mathbf{f}_i$ and the j-th receive beam $\mathbf{w}_j$ is captured by the product $\mathbf{w}_j^* \mathbf{H} \mathbf{f}_i$, which can be extended to encompass all transmit-receive beam pairs as $\mathbf{W}^* \mathbf{H} \mathbf{F} \in \mathbb{C}^{M_{\text{rx}} \times M_{\text{tx}}}$. LONESTAR will aim to minimize the coupling across all beam pairs and does so by minimizing

the average $\mathsf{INR}_{\mathrm{rx}}$ coupled between beam pairs, which can be written as

$$\mathsf{INR}_{\mathrm{rx}}^{\mathrm{avg}} = \frac{1}{M_{\mathrm{tx}} \cdot M_{\mathrm{rx}}} \cdot \sum_{i=1}^{M_{\mathrm{tx}}} \sum_{j=1}^{M_{\mathrm{rx}}} \frac{P_{\mathrm{tx}}^{\mathrm{BS}} \cdot G^2 \cdot \left|\mathbf{w}_j^* \mathbf{H} \mathbf{f}_i\right|^2}{N_{\mathrm{t}} \cdot \|\mathbf{w}_j\|_2^2 \cdot P_{\mathrm{noise}}^{\mathrm{BS}}} \tag{19}$$

$$\approx \frac{P_{\mathrm{tx}}^{\mathrm{BS}} \cdot G^2}{N_{\mathrm{t}} \cdot N_{\mathrm{r}} \cdot P_{\mathrm{noise}}^{\mathrm{BS}}} \cdot \frac{\|\mathbf{W}^* \mathbf{H} \mathbf{F}\|_{\mathrm{F}}^2}{M_{\mathrm{tx}} \cdot M_{\mathrm{rx}}}, \tag{20}$$

where the approximation becomes equality when $\|\mathbf{w}_j\|_2^2 = N_{\mathrm{r}}$ for all j. Minimizing $\mathsf{INR}_{\mathrm{rx}}^{\mathrm{avg}}$ can be accomplished (approximately) by minimizing $\|\mathbf{W}^* \mathbf{H} \mathbf{F}\|_{\mathrm{F}}^2$ through the design of $\mathbf{F}$ and $\mathbf{W}$ for a given $\mathbf{H}$ since all other terms are constants. In LONESTAR's attempt to minimize $\mathsf{INR}_{\mathrm{rx}}^{\mathrm{avg}}$, it must also ensure that the beams in $\mathbf{F}$ and $\mathbf{W}$ remain useful in serving users; of course, $\mathbf{F}$ and $\mathbf{W}$ minimize $\mathsf{INR}_{\mathrm{rx}}^{\mathrm{avg}}$ when driven to $\mathbf{0}$ if unconstrained. We now quantify a means to constrain LONESTAR to ensure adequate service is maintained in its aim to minimize $\mathsf{INR}_{\mathrm{rx}}^{\mathrm{avg}}$.

Definition 5: Transmit and receive coverage variances. To offer flexibility in minimizing $\mathsf{INR}_{\mathrm{rx}}^{\mathrm{avg}}$, LONESTAR tolerates some sacrifices in beamforming gain over the transmit and receive coverage regions. In other words, we allow for transmit and receive beamforming gains less than N_{t}^2 and N_{r}^2 over $\mathcal{A}_{\mathrm{tx}}$ and $\mathcal{A}_{\mathrm{rx}}$ in pursuit of reduced self-interference. Let $\sigma_{\mathrm{tx}}^2 \geq 0$ be the maximum variance tolerated in delivering maximum transmit gain across $\mathcal{A}_{\mathrm{tx}}$, normalized to N_{t}^2. Defining $\sigma_{\mathrm{rx}}^2 \geq 0$ analogously, we express these tolerated coverage variances as

$$\frac{1}{M_{\mathrm{tx}}} \cdot \sum_{i=1}^{M_{\mathrm{tx}}} \frac{\left|N_{\mathrm{t}} - g_{\mathrm{tx}}\left(\theta_{\mathrm{tx}}^{(i)}\right)\right|^2}{N_{\mathrm{t}}^2} \leq \sigma_{\mathrm{tx}}^2, \tag{21}$$

$$\frac{1}{M_{\mathrm{rx}}} \cdot \sum_{j=1}^{M_{\mathrm{rx}}} \frac{\left|N_{\mathrm{r}} - g_{\mathrm{rx}}\left(\theta_{\mathrm{rx}}^{(j)}\right)\right|^2}{N_{\mathrm{r}}^2} \leq \sigma_{\mathrm{rx}}^2. \tag{22}$$

Here, σ_{tx}^2 and σ_{rx}^2 are design parameters that can be tuned by system engineers; increasing them will offer LONESTAR greater flexibility in reducing $\mathsf{INR}_{\mathrm{rx}}^{\mathrm{avg}}$ but may degrade coverage since it permits more variability in beamforming gain over the service regions.

B. Assembling Our Codebook Design Problem

In the previous subsection, we outlined that LONESTAR will attempt to minimize the average self-interference coupled by transmit and receive beams while constraining the variance of beamforming gain delivered to specified transmit and receive coverage regions. With expressions for our codebook design criteria in hand, we now turn our attention to assembling a formal design problem. Let $\mathbf{A}_{\mathrm{tx}} \in \mathbb{C}^{N_{\mathrm{t}} \times M_{\mathrm{tx}}}$ be the matrix of transmit array response vectors evaluated at the directions in $\mathcal{A}_{\mathrm{tx}}$, and let $\mathbf{A}_{\mathrm{rx}} \in \mathbb{C}^{N_{\mathrm{r}} \times M_{\mathrm{rx}}}$ be defined analogously.

$$\mathbf{A}_{\mathrm{tx}} = \left[\mathbf{a}_{\mathrm{tx}}\left(\theta_{\mathrm{tx}}^{(1)}\right) \quad \mathbf{a}_{\mathrm{tx}}\left(\theta_{\mathrm{tx}}^{(2)}\right) \quad \cdots \quad \mathbf{a}_{\mathrm{tx}}\left(\theta_{\mathrm{tx}}^{(M_{\mathrm{tx}})}\right)\right] \tag{23}$$

$$\mathbf{A}_{\mathrm{rx}} = \left[\mathbf{a}_{\mathrm{rx}}\left(\theta_{\mathrm{rx}}^{(1)}\right) \quad \mathbf{a}_{\mathrm{rx}}\left(\theta_{\mathrm{rx}}^{(2)}\right) \quad \cdots \quad \mathbf{a}_{\mathrm{rx}}\left(\theta_{\mathrm{rx}}^{(M_{\mathrm{rx}})}\right)\right] \tag{24}$$

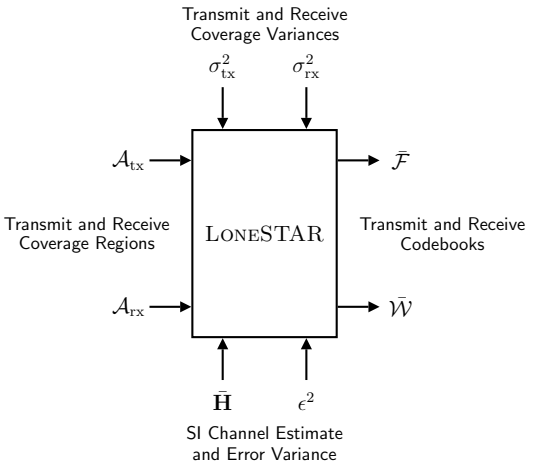

Fig. 4. Using an estimate of the self-interference channel and knowledge of the estimation error variance, LONESTAR produces transmit and receive beamforming codebooks that serve some coverage regions with quality based on tolerated coverage variances.

Recall, these can be computed directly based on the transmit and receive array geometries [5], [33]. Using these, the expressions of (21) and (22) can be written equivalently (up to arbitrary phase shifts of $\mathbf{f}_i$ and $\mathbf{w}_j$) as follows, which we refer to as *coverage constraints*.

$$\|N_{\mathrm{t}} \cdot \mathbf{1} - \mathrm{diag}(\mathbf{A}_{\mathrm{tx}}^* \mathbf{F})\|_2^2 \leq \sigma_{\mathrm{tx}}^2 \cdot N_{\mathrm{t}}^2 \cdot M_{\mathrm{tx}} \tag{25}$$

$$\|N_{\mathrm{r}} \cdot \mathbf{1} - \mathrm{diag}(\mathbf{A}_{\mathrm{rx}}^* \mathbf{W})\|_2^2 \leq \sigma_{\mathrm{rx}}^2 \cdot N_{\mathrm{r}}^2 \cdot M_{\mathrm{rx}} \tag{26}$$

Note that the (i,i)-th entry of $\mathbf{A}_{\mathrm{tx}}^* \mathbf{F}$ has magnitude $g_{\mathrm{tx}}\left(\theta_{\mathrm{tx}}^{(i)}\right)$ and the (j,j)-th entry of $\mathbf{A}_{\mathrm{rx}}^* \mathbf{W}$ has magnitude $g_{\mathrm{rx}}\left(\theta_{\mathrm{rx}}^{(j)}\right)$. By satisfying (25) and (26), engineers can ensure that LONESTAR codebooks adequately serve their coverage regions for appropriately chosen σ_{tx}^2 and σ_{rx}^2.

With coverage constraints (25) and (26), we now formulate an analog beamforming codebook design in problem (27). The goal of LONESTAR is to design transmit and receive codebooks that minimize the self-interference coupled between each transmit and receive beam pair while ensuring the codebooks remain useful in delivering service to users.

$$\min_{\mathbf{F},\mathbf{W}} \quad \|\mathbf{W}^* \mathbf{H} \mathbf{F}\|_{\mathrm{F}}^2 \tag{27a}$$

$$\text{s.t.} \quad \|N_{\mathrm{t}} \cdot \mathbf{1} - \mathrm{diag}(\mathbf{A}_{\mathrm{tx}}^* \mathbf{F})\|_2^2 \leq \sigma_{\mathrm{tx}}^2 \cdot N_{\mathrm{t}}^2 \cdot M_{\mathrm{tx}} \tag{27b}$$

$$\|N_{\mathrm{r}} \cdot \mathbf{1} - \mathrm{diag}(\mathbf{A}_{\mathrm{rx}}^* \mathbf{W})\|_2^2 \leq \sigma_{\mathrm{rx}}^2 \cdot N_{\mathrm{r}}^2 \cdot M_{\mathrm{rx}} \tag{27c}$$

$$[\mathbf{F}]_{:,i} \in \mathcal{F} \ \forall \ i = 1, \ldots, M_{\mathrm{tx}} \tag{27d}$$

$$[\mathbf{W}]_{:,j} \in \mathcal{W} \ \forall \ j = 1, \ldots, M_{\mathrm{rx}} \tag{27e}$$

By minimizing the Frobenius norm in the objective, our designed codebooks aim to minimize the average self-interference coupled across all transmit-receive beam pairs as evident in (20). While doing so, our codebooks must satisfy the coverage constraints (27b) and (27c) that were established in (25) and (26). Constraints (27d) and (27e) require our design to create codebooks whose beams are physically realizable with digitally-controlled phase shifters and attenuators.

Practical systems cannot solve problem (27) since they do not have knowledge of the true self-interference channel $\mathbf{H}$ but

rather the estimate $\bar{\mathbf{H}}$. This motivates us to modify problem (27) to incorporate robustness to channel estimation error. It is common in robust communication system optimization to minimize the worst-case error inflicted by some uncertainty [35]–[38]. In our case, $\boldsymbol{\Delta}$ has i.i.d. Gaussian entries, meaning the worst-case error inflicted on the objective of problem (27) is unbounded. In light of this, we instead minimize the expectation of our objective over the distribution of $\mathbf{H}$. Forming problem (28), LONESTAR aims to minimize the expected average self-interference coupled between beam pairs, given some estimate $\bar{\mathbf{H}}$.

$$\min_{\mathbf{F},\mathbf{W}} \quad \mathop{\mathbb{E}}_{\mathbf{H}}\left[\|\mathbf{W}^*\mathbf{H}\mathbf{F}\|_{\mathrm{F}}^2 \mid \bar{\mathbf{H}}\right] \tag{28a}$$

$$\text{s.t.} \quad \|N_{\mathrm{t}}\cdot\mathbf{1}-\mathrm{diag}(\mathbf{A}_{\mathrm{tx}}^*\mathbf{F})\|_2^2 \le \sigma_{\mathrm{tx}}^2\cdot N_{\mathrm{t}}^2\cdot M_{\mathrm{tx}} \tag{28b}$$

$$\|N_{\mathrm{r}}\cdot\mathbf{1}-\mathrm{diag}(\mathbf{A}_{\mathrm{rx}}^*\mathbf{W})\|_2^2 \le \sigma_{\mathrm{rx}}^2\cdot N_{\mathrm{r}}^2\cdot M_{\mathrm{rx}} \tag{28c}$$

$$[\mathbf{F}]_{:,i}\in\mathcal{F}\ \forall\ i=1,\dots,M_{\mathrm{tx}} \tag{28d}$$

$$[\mathbf{W}]_{:,j}\in\mathcal{W}\ \forall\ j=1,\dots,M_{\mathrm{rx}} \tag{28e}$$

To transform problem (28) into one we can more readily solve, we derive a closed-form expression of the objective (28a), courtesy of the fact that $\boldsymbol{\Delta}$ is Gaussian.

Theorem 1. *The objective of problem* (28) *is equivalent to*

$$\mathop{\mathbb{E}}_{\mathbf{H}}\left[\|\mathbf{W}^*\mathbf{H}\mathbf{F}\|_{\mathrm{F}}^2 \mid \bar{\mathbf{H}}\right] = \left\|\mathbf{W}^*\bar{\mathbf{H}}\mathbf{F}\right\|_{\mathrm{F}}^2 + \epsilon^2\cdot\|\mathbf{F}\|_{\mathrm{F}}^2\cdot\|\mathbf{W}\|_{\mathrm{F}}^2. \tag{29}$$

Proof. We begin by recalling (12) to write

$$\mathop{\mathbb{E}}_{\mathbf{H}}\left[\|\mathbf{W}^*\mathbf{H}\mathbf{F}\|_{\mathrm{F}}^2 \mid \bar{\mathbf{H}}\right] \tag{30}$$

$$= \mathop{\mathbb{E}}_{\boldsymbol{\Delta}}\left[\left\|\mathbf{W}^*\big(\bar{\mathbf{H}}+\boldsymbol{\Delta}\big)\mathbf{F}\right\|_{\mathrm{F}}^2\right] \tag{31}$$

$$\overset{(a)}{=} \mathop{\mathbb{E}}_{\boldsymbol{\Delta}}\left[\mathrm{tr}\Big(\big(\mathbf{W}^*\big(\bar{\mathbf{H}}+\boldsymbol{\Delta}\big)\mathbf{F}\big)\big(\mathbf{W}^*\big(\bar{\mathbf{H}}+\boldsymbol{\Delta}\big)\mathbf{F}\big)^*\Big)\right] \tag{32}$$

$$\overset{(b)}{=} \left\|\mathbf{W}^*\bar{\mathbf{H}}\mathbf{F}\right\|_{\mathrm{F}}^2 + \mathrm{tr}\Big(\mathbf{F}^*\mathop{\mathbb{E}}_{\boldsymbol{\Delta}}[\boldsymbol{\Delta}^*\mathbf{W}\mathbf{W}^*\boldsymbol{\Delta}]\mathbf{F}\Big) \tag{33}$$

$$\overset{(c)}{=} \left\|\mathbf{W}^*\bar{\mathbf{H}}\mathbf{F}\right\|_{\mathrm{F}}^2 + \mathrm{tr}\Big(\mathbf{F}^*\mathop{\mathbb{E}}_{\boldsymbol{\Delta}}[\boldsymbol{\Delta}^*\mathbf{U}_{\mathbf{W}}\boldsymbol{\Lambda}_{\mathbf{W}}\mathbf{U}_{\mathbf{W}}^*\boldsymbol{\Delta}]\mathbf{F}\Big) \tag{34}$$

$$\overset{(d)}{=} \left\|\mathbf{W}^*\bar{\mathbf{H}}\mathbf{F}\right\|_{\mathrm{F}}^2 + \mathrm{tr}\left(\mathbf{F}^*\mathop{\mathbb{E}}_{\tilde{\boldsymbol{\Delta}}}\left[\tilde{\boldsymbol{\Delta}}\boldsymbol{\Lambda}_{\mathbf{W}}\tilde{\boldsymbol{\Delta}}^*\right]\mathbf{F}\right) \tag{35}$$

$$\overset{(e)}{=} \left\|\mathbf{W}^*\bar{\mathbf{H}}\mathbf{F}\right\|_{\mathrm{F}}^2 + \mathrm{tr}(\mathbf{F}^*\mathbf{F})\cdot\epsilon^2\cdot\mathrm{tr}(\boldsymbol{\Lambda}_{\mathbf{W}}) \tag{36}$$

$$\overset{(f)}{=} \left\|\mathbf{W}^*\bar{\mathbf{H}}\mathbf{F}\right\|_{\mathrm{F}}^2 + \epsilon^2\cdot\|\mathbf{F}\|_{\mathrm{F}}^2\cdot\|\mathbf{W}\|_{\mathrm{F}}^2 \tag{37}$$

where (a) follows from $\|\mathbf{A}\|_{\mathrm{F}}^2 = \mathrm{tr}(\mathbf{A}\mathbf{A}^*)$; (b) is by the linearity of expectation and trace and the fact that $\mathbb{E}[\boldsymbol{\Delta}]=\mathbf{0}$; (c) is by taking the eigenvalue decomposition $\mathbf{W}\mathbf{W}^* = \mathbf{U}_{\mathbf{W}}\boldsymbol{\Lambda}_{\mathbf{W}}\mathbf{U}_{\mathbf{W}}^*$; (d) is by defining $\tilde{\boldsymbol{\Delta}} = \boldsymbol{\Delta}^*\mathbf{U}_{\mathbf{W}}$, which has the same distribution as $\boldsymbol{\Delta}$ by unitary invariance of i.i.d. zero-mean Gaussian matrices [5]; (e) is via the property [39]

$$\mathop{\mathbb{E}}_{\mathbf{X}}[\mathbf{X}\mathbf{A}\mathbf{X}^*] = \epsilon^2\cdot\mathrm{tr}(\mathbf{A}^*)\cdot\mathbf{I}, \tag{38}$$

where $\mathbf{X}$ has entries i.i.d. Gaussian with mean 0 and variance ϵ^2; and (f) follows from the definition of Frobenius norm. □

Using Theorem 1, problem (28) can be rewritten equivalently as follows.

$$\min_{\mathbf{F},\mathbf{W}} \quad \left\|\mathbf{W}^*\bar{\mathbf{H}}\mathbf{F}\right\|_{\mathrm{F}}^2 + \epsilon^2\cdot\|\mathbf{F}\|_{\mathrm{F}}^2\cdot\|\mathbf{W}\|_{\mathrm{F}}^2 \tag{39a}$$

$$\text{s.t.} \quad \|N_{\mathrm{t}}\cdot\mathbf{1}-\mathrm{diag}(\mathbf{A}_{\mathrm{tx}}^*\mathbf{F})\|_2^2 \le \sigma_{\mathrm{tx}}^2\cdot N_{\mathrm{t}}^2\cdot M_{\mathrm{tx}} \tag{39b}$$

$$\|N_{\mathrm{r}}\cdot\mathbf{1}-\mathrm{diag}(\mathbf{A}_{\mathrm{rx}}^*\mathbf{W})\|_2^2 \le \sigma_{\mathrm{rx}}^2\cdot N_{\mathrm{r}}^2\cdot M_{\mathrm{rx}} \tag{39c}$$

$$[\mathbf{F}]_{:,i}\in\mathcal{F}\ \forall\ i=1,\dots,M_{\mathrm{tx}} \tag{39d}$$

$$[\mathbf{W}]_{:,j}\in\mathcal{W}\ \forall\ j=1,\dots,M_{\mathrm{rx}} \tag{39e}$$

For some channel estimate $\bar{\mathbf{H}}$ and knowledge of the estimation error variance ϵ^2, engineers can aim to solve problem (39) for codebooks $\mathbf{F}$ and $\mathbf{W}$ that minimize the expected average self-interference coupled between transmit and receive beams while ensuring coverage is delivered with some quality parameterized by σ_{tx}^2 and σ_{rx}^2. This concludes the formulation of our codebook design LONESTAR. In the next section, we present a means to solve problem (39), along with a summary of and commentary on our design.

V. SOLVING FOR LONESTAR CODEBOOKS AND DESIGN REMARKS

In the previous section, we formulated problem (39), a codebook design problem that accounts for self-interference channel estimation error and digitally-controlled phase shifters and attenuators. In this section, we present an approach for (approximately) solving this design problem using a projected alternating minimization approach. We conclude this section with a summary of our design and remarks regarding design decisions.

Problem (39) cannot be efficiently solved directly due to the non-convexity posed by digitally-controlled phase shifters and attenuators (i.e., $\mathcal{F}$ and $\mathcal{W}$ are non-convex sets). The joint optimization of $\mathbf{F}$ and $\mathbf{W}$ introduces further complexity, especially given their dimensionality. In order to approximately but efficiently solve problem (39), we take a projected alternating minimization approach, which is summarized in Algorithm 1. Let $\Pi_{\mathcal{F}}\Big([\mathbf{F}]_{:,i}\Big)$ be the projection of the i-th beam (column) of $\mathbf{F}$ onto the set of physically realizable beamforming vectors $\mathcal{F}$. We extend this projection onto each beam in $\mathbf{F}$ as $\Pi_{\mathcal{F}}(\mathbf{F})$ by applying it column-wise on $\mathbf{F}$; the projection of $\mathbf{W}$ onto $\mathcal{W}$ is defined analogously. With digitally-controlled phase shifters and attenuators, each element of $\mathbf{F}$ must be quantized in both phase and amplitude. Since the set of physically realizable beamforming weights is the same for each element in a beamforming vector, the projection of that vector reduces to projecting each of its elements. The (m,n)-th element following the projection of $\mathbf{F}$ onto $\mathcal{F}$ can be expressed as

$$[\Pi_{\mathcal{F}}(\mathbf{F})]_{m,n} = A^\star\cdot\exp(\mathrm{j}\cdot\theta^\star), \tag{40}$$

where $A^\star$ and $\theta^\star$ are the quantized amplitude and phase of $[\mathbf{F}]_{m,n}$. These can be expressed as

$$A^\star = \mathop{\mathrm{argmin}}_{A_i\in\mathcal{A}} |A_i - A|, \tag{41}$$

$$\theta^\star = \mathop{\mathrm{argmin}}_{\theta_i\in\mathcal{P}} |\exp(\mathrm{j}\cdot\theta_i) - \exp(\mathrm{j}\cdot\theta)|, \tag{42}$$

where $A = \left|[\mathbf{F}]_{m,n}\right|$ and $\theta = \text{angle}\left([\mathbf{F}]_{m,n}\right)$ are the magnitude and phase of $[\mathbf{F}]_{m,n}$. Here, $\mathcal{A}$ and $\mathcal{P}$ are the sets of physically realizable amplitudes (attenuator settings) and phases (phase shifter settings), respectively.

To approximately solve problem (39), we begin with $\mathbf{F} \leftarrow \Pi_{\mathcal{F}}(\mathbf{A}_{\text{tx}})$ and $\mathbf{W} \leftarrow \Pi_{\mathcal{W}}(\mathbf{A}_{\text{rx}})$, which initializes our beams as matched filters to achieve (near) maximum gains across $\mathcal{A}_{\text{tx}}$ and $\mathcal{A}_{\text{rx}}$, respectively. Then, we fix the receive codebook $\mathbf{W}$ and solve problem (43) below.

$$\min_{\mathbf{F}} \quad \left\|\mathbf{W}^*\bar{\mathbf{H}}\mathbf{F}\right\|_{\text{F}}^2 + \epsilon^2 \cdot \|\mathbf{F}\|_{\text{F}}^2 \cdot \|\mathbf{W}\|_{\text{F}}^2 \tag{43a}$$

$$\text{s.t.} \quad \|N_{\text{t}} \cdot \mathbf{1} - \text{diag}(\mathbf{A}_{\text{tx}}^*\mathbf{F})\|_2^2 \leq \sigma_{\text{tx}}^2 \cdot N_{\text{t}}^2 \cdot M_{\text{tx}} \tag{43b}$$

$$\left|[\mathbf{F}]_{i,j}\right| \leq 1, \ i = 1, \ldots, N_{\text{t}}, \ j = 1, \ldots, M_{\text{tx}} \tag{43c}$$

As a temporary convex relaxation, we have introduced constraint (43c) instead of requiring strict quantized phase and amplitude control. This enforces that each beamforming weight not exceed unit magnitude, understood by the fact that attenuators are used for amplitude control as outlined in (1) and (2). Problem (43) is convex and can be readily solved using convex optimization solvers (e.g., we used [40]). Dedicated algorithms more efficient than general solvers can likely be developed for LONESTAR, but that is beyond the scope of this work, making it a good topic for future work. After solving problem (43), the solution $\mathbf{F}^\star$ is projected onto the set $\mathcal{F}$ as $\mathbf{F} \leftarrow \Pi_{\mathcal{F}}(\mathbf{F}^\star)$ to ensure it is physically realizable. The projected $\mathbf{F}$ is then used when solving for the receive codebook in problem (44) below.

$$\min_{\mathbf{W}} \quad \left\|\mathbf{W}^*\bar{\mathbf{H}}\mathbf{F}\right\|_{\text{F}}^2 + \epsilon^2 \cdot \|\mathbf{F}\|_{\text{F}}^2 \cdot \|\mathbf{W}\|_{\text{F}}^2 \tag{44a}$$

$$\text{s.t.} \quad \|N_{\text{r}} \cdot \mathbf{1} - \text{diag}(\mathbf{A}_{\text{rx}}^*\mathbf{W})\|_2^2 \leq \sigma_{\text{rx}}^2 \cdot N_{\text{r}}^2 \cdot M_{\text{rx}} \tag{44b}$$

$$\left|[\mathbf{W}]_{i,j}\right| \leq 1, \ i = 1, \ldots, N_{\text{r}}, \ j = 1, \ldots, M_{\text{rx}} \tag{44c}$$

Problem (44) has a form identical to problem (43) and is thus convex and can be solved using the same approach used for problem (43). Upon solving problem (44), we ensure the solution $\mathbf{W}^\star$ is physically realizable by projecting it onto $\mathcal{W}$ via $\mathbf{W} \leftarrow \Pi_{\mathcal{W}}(\mathbf{W}^\star)$. This alternating minimization is only executed once since convergence is typically reached immediately due to limited phase and amplitude control; in other words, additional iterations simply project on to the same solutions as the first solution. This concludes our design of LONESTAR, which has produced physically realizable transmit and receive codebook matrices $\mathbf{F}$ and $\mathbf{W}$. These can then be unpacked via Definition 2 to form the sets $\bar{\mathcal{F}}$ and $\bar{\mathcal{W}}$ that can be used for beam alignment and subsequent full-duplexing of downlink and uplink. In the next two sections, we evaluate LONESTAR extensively through simulation.

Remark 1: Design decisions. We present a summary of LONESTAR in Algorithm 2, and now provide a few remarks on our approach and communicate our motivations and design decisions. The objective of LONESTAR is to create transmit and receive codebooks that minimize the average INR_{rx} while still delivering high transmit and receive beamforming gain. It may seem preferred to maximize the average $\mathsf{SINR}_{\text{rx}}$ or sum spectral efficiency, but this requires knowledge of the transmit and receive SNRs, which the system only has *after* conducting beam alignment, or real-time knowledge of $\mathbf{h}_{\text{tx}}$ and $\mathbf{h}_{\text{rx}}$, which is currently impractical. LONESTAR only relies on knowledge of the self-interference MIMO channel and not that of the transmit and receive channels. By minimizing INR_{rx} while constraining transmit and receive coverage quality (i.e., maintaining high SNR_{tx} and SNR_{rx}), LONESTAR can consequently achieve high $\mathsf{SINR}_{\text{rx}}$ and $\mathsf{SINR}_{\text{tx}}$. One may also suggest we instead minimize the codebooks' maximum INR_{rx} (to minimize worst-case self-interference) rather than minimize the average INR_{rx}. We chose to minimize the average INR_{rx} because this prevents LONESTAR from being significantly hindered if there are select transmit-receive beam pairs that simply cannot offer low self-interference while delivering high beamforming gain. It is important to note that the Frobenius norm objective used by LONESTAR will make it more incentivized to reduce high self-interference but does not exclusively prioritize worst-case beam pairs [35]. Individual beam pairs that do not yield sufficiently low INR_{rx} when minimizing the average INR_{rx} with LONESTAR could potentially be avoided via scheduling or half-duplexed as a last resort.

Algorithm 1 Projected alternating minimization to approximately solve problem (39).

1. Initialize $\mathbf{F} \leftarrow \Pi_{\mathcal{F}}(\mathbf{A}_{\text{tx}})$ and $\mathbf{W} \leftarrow \Pi_{\mathcal{W}}(\mathbf{A}_{\text{rx}})$.
2. Solve problem (43) for the transmit codebook $\mathbf{F}^\star$.
3. Project $\mathbf{F}^\star$ to ensure it is physically realizable: $\mathbf{F} \leftarrow \Pi_{\mathcal{F}}(\mathbf{F}^\star)$.
4. Solve problem (44) for the receive codebook $\mathbf{W}^\star$ using the updated $\mathbf{F}$.
5. Project $\mathbf{W}^\star$ to ensure it is physically realizable: $\mathbf{W} \leftarrow \Pi_{\mathcal{W}}(\mathbf{W}^\star)$.

Remark 2: Complexity. It is difficult to comment on the complexity of our design for a few reasons. First and foremost, its complexity depends heavily on the solver used for solving problems (43) and (44). As mentioned, more efficient solving algorithms may be tailored for LONESTAR, but that is out of the scope of this work. Additionally, total computational costs will depend on the initialization of $\mathbf{F}$ and $\mathbf{W}$. We have initialized them both as conjugate beamforming codebooks; in practice, it would likely be efficient to use previous solutions of $\mathbf{F}$ and $\mathbf{W}$ when rerunning LONESTAR to account for drift in the self-interference channel. Note that our design takes place at the full-duplex BS, which presumably has sufficient compute resources to execute LONESTAR. Practically, it may be preferred to conduct a thorough estimation of $\mathbf{H}$ and execution of LONESTAR during initial setup of the BS and then perform updates to the estimate of $\mathbf{H}$ and possibly to our design over time; this would be interesting future work. Most existing beamforming-based full-duplex solutions need to be executed for each downlink-uplink user pair, whereas the same LONESTAR design can be used across many user pairs, meaning it may offer significant computational savings in comparison.

Algorithm 2 A summary of our analog beamforming codebook design, LONESTAR.

1. Obtain an estimate $\bar{\mathbf{H}}$ of the self-interference channel and the estimation error variance ϵ^2.
2. Define transmit and receive coverage regions $\mathcal{A}_{\mathrm{tx}}$ and $\mathcal{A}_{\mathrm{rx}}$ and assemble $\mathbf{A}_{\mathrm{tx}}$ and $\mathbf{A}_{\mathrm{rx}}$.
3. Set transmit and receive coverage variances σ^2_{tx} and σ^2_{rx}.
4. Solve problem (39) for $\mathbf{F}$ and $\mathbf{W}$ using Algorithm 1.
5. Unpack $\mathbf{F}$ and $\mathbf{W}$ to form codebooks $\bar{\mathcal{F}}$ and $\bar{\mathcal{W}}$ using Definition 2.

VI. SIMULATION SETUP AND PERFORMANCE METRICS

We simulated the full-duplex system illustrated in Fig. 1 at 30 GHz in a Monte Carlo fashion to extensively evaluate LONESTAR against conventional codebooks [41]. The full-duplex BS is equipped with two 8×8 half-wavelength uniform planar arrays for transmission and reception; users have a single antenna for simplicity. Analog beamforming networks at the BS use log-stepped attenuators with 0.5 dB of attenuation per least significant bit (LSB) and phase shifters with uniform phase control over $[0, 2\pi)$. We consider downlink and uplink service regions spanning -60° to 60° in azimuth and -30° to 30° in elevation, each in 15° steps, resulting in codebooks of $M_{\mathrm{tx}} = M_{\mathrm{rx}} = 45$ beams. Users are distributed uniformly from -67.5° to 67.5° in azimuth and from -37.5° to 37.5° in elevation. The downlink and uplink channels are simulated as line-of-sight (LOS) channels for simplicity; similar conclusions would be expected when modeling them otherwise due to the directional nature of mmWave channels. To select which transmit and receive beams serve a given downlink and uplink user pair, we use exhaustive beam sweeping on each link independently and choose the beams that maximize $\mathsf{SNR}_{\mathrm{tx}}$ and $\mathsf{SNR}_{\mathrm{rx}}$. The choice of a particular self-interference channel model is a difficult one to justify practically, given there lacks a well-accepted, measurement-backed model. We have chosen to simulate the self-interference channel $\mathbf{H}$ using the spherical-wave channel model [42], which captures idealized near-field propagation between the transmit and receive arrays of the full-duplex device and has been used widely thus far in the related literature. This channel model is a function of the relative geometry between the transmit and receive arrays and is defined as

$$[\mathbf{H}]_{m,n} = \frac{\rho}{r_{n,m}} \exp\Big(-\mathrm{j}2\pi \frac{r_{n,m}}{\lambda}\Big), \tag{45}$$

where $r_{n,m}$ is the distance between the n-th transmit antenna and the m-th receive antenna, λ is the carrier wavelength, and ρ is a normalizing factor to satisfy $\|\mathbf{H}\|_{\mathrm{F}}^2 = N_{\mathrm{t}} \cdot N_{\mathrm{r}}$. To realize such a channel, we have vertically stacked our transmit and receive arrays with 10λ of separation. While this channel model may not hold perfectly in practice, it provides a sensible starting point to evaluate LONESTAR, particularly when self-interference is dominated by idealized near-field propagation. Shortly, for more extensive evaluation, we consider a self-interference channel model that mixes this spherical-wave model with a Rayleigh faded channel. We do not model cross-link interference explicitly but instead evaluate performance over various $\mathsf{INR}_{\mathrm{tx}}$.

A. Baselines and Performance Metrics

Considering LONESTAR is the first known codebook design specifically for mmWave full-duplex, we evaluate it against two conventional codebooks, both of which are used in practice by half-duplex systems to form sets of beams that provide broad coverage with high gain:

- A *CBF codebook* that uses conjugate beamforming [5], where
$$\mathbf{f}_i = \Pi_{\mathcal{F}}\Big(\mathbf{a}_{\mathrm{tx}}\Big(\theta^{(i)}_{\mathrm{tx}}\Big)\Big), \quad \mathbf{w}_j = \Pi_{\mathcal{W}}\Big(\mathbf{a}_{\mathrm{rx}}\Big(\theta^{(j)}_{\mathrm{rx}}\Big)\Big). \tag{46}$$
CBF codebooks can deliver (approximately) maximum gain to all directions in $\mathcal{A}_{\mathrm{tx}}$ and $\mathcal{A}_{\mathrm{rx}}$. The projections here are simply to ensure the beams are physically realizable and do not have significant impacts on the beam shapes with modest phase shifter resolution b_{phs}.
- A *Taylor codebook* that uses conjugate beamforming with side lobe suppression as
$$\mathbf{f}_i = \Pi_{\mathcal{F}}\Big(\mathbf{a}_{\mathrm{tx}}\Big(\theta^{(i)}_{\mathrm{tx}}\Big) \odot \mathbf{v}_{\mathrm{tx}}\Big), \tag{47}$$
$$\mathbf{w}_j = \Pi_{\mathcal{W}}\Big(\mathbf{a}_{\mathrm{rx}}\Big(\theta^{(j)}_{\mathrm{rx}}\Big) \odot \mathbf{v}_{\mathrm{rx}}\Big), \tag{48}$$
where $\mathbf{v}_{\mathrm{tx}}$ and $\mathbf{v}_{\mathrm{rx}}$ are Taylor windows applied element-wise, providing 25 dB of side lobe suppression; we found this level of side lobe suppression competes best with LONESTAR. Taylor windowing is an established means to reduce interference inflicted by side lobe levels at the cost of lessened beamforming gain and a wider main lobe [7], [8].

We assess LONESTAR against our baseline codebooks in terms of spectral efficiency of the transmit and receive links. Specifically, we use the normalized sum spectral efficiency

$$\gamma_{\mathrm{sum}} = \frac{R_{\mathrm{tx}} + R_{\mathrm{rx}}}{C^{\mathrm{cb}}_{\mathrm{tx}} + C^{\mathrm{cb}}_{\mathrm{rx}}}, \tag{49}$$

where $C^{\mathrm{cb}}_{\mathrm{tx}} = \log_2\Big(1 + \mathsf{SNR}^{\mathrm{CBF}}_{\mathrm{tx}}\Big)$ and $C^{\mathrm{cb}}_{\mathrm{rx}} = \log_2\Big(1 + \mathsf{SNR}^{\mathrm{CBF}}_{\mathrm{rx}}\Big)$ we term the *codebook capacities*; here, $\mathsf{SNR}^{\mathrm{CBF}}_{\mathrm{tx}}$ and $\mathsf{SNR}^{\mathrm{CBF}}_{\mathrm{rx}}$ are the maximum SNRs delivered to a given downlink-uplink user pair by the CBF codebook. In other words, $C^{\mathrm{cb}}_{\mathrm{tx}} + C^{\mathrm{cb}}_{\mathrm{rx}}$ is the maximum sum spectral efficiency when using the CBF codebook and interference is inherently not present (i.e., when $\overline{\mathsf{INR}}_{\mathrm{rx}} = \mathsf{INR}_{\mathrm{tx}} = -\infty$ dB). With this normalization, γ_{sum} will gauge how well a given codebook delivers transmission and reception in the face of self-interference and cross-link interference, relative to the interference-free capacity when beamforming with the CBF codebook. Note that $\gamma_{\mathrm{sum}} = 0.5$ can be achieved with the CBF codebook by half-duplexing transmission and reception with equal time-division duplexing (TDD) under an instantaneous power constraint. As such, LONESTAR generally aims to exceed $\gamma_{\mathrm{sum}} = 0.5$ and outperform that achieved by CBF and Taylor codebooks. Note that γ_{sum} is not truly upper-bounded by 1 since $C^{\mathrm{cb}}_{\mathrm{tx}} + C^{\mathrm{cb}}_{\mathrm{rx}}$ is not the true sum Shannon capacity; nonetheless, achieving $\gamma_{\mathrm{sum}} \approx 1$ indicates

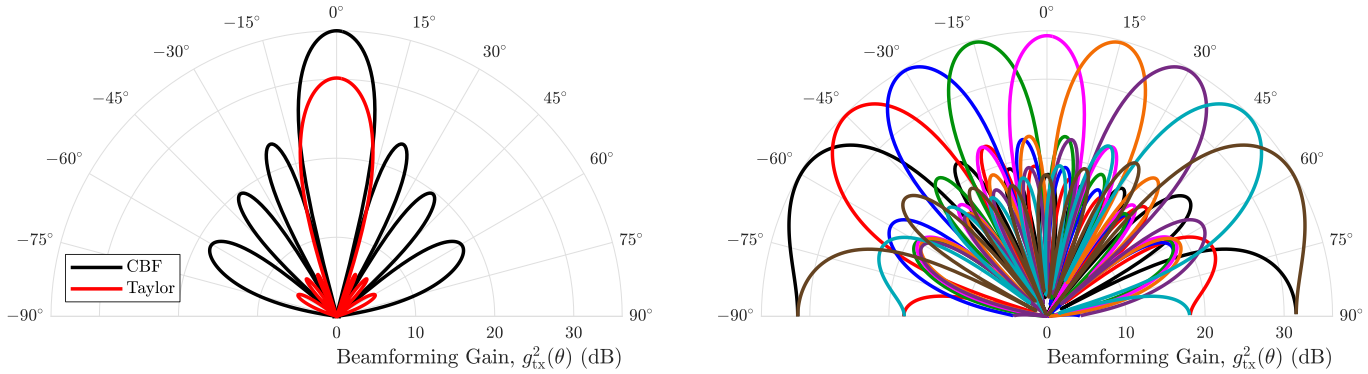

(a) Conventional broadside beams.

(b) LoneSTAR beams.

Fig. 5. (a) The azimuth cut of a broadside beam from conventional CBF and Taylor codebooks. (b) The azimuth cuts of transmit beams produced by LoneSTAR that serve various azimuth directions at an elevation of 0°.

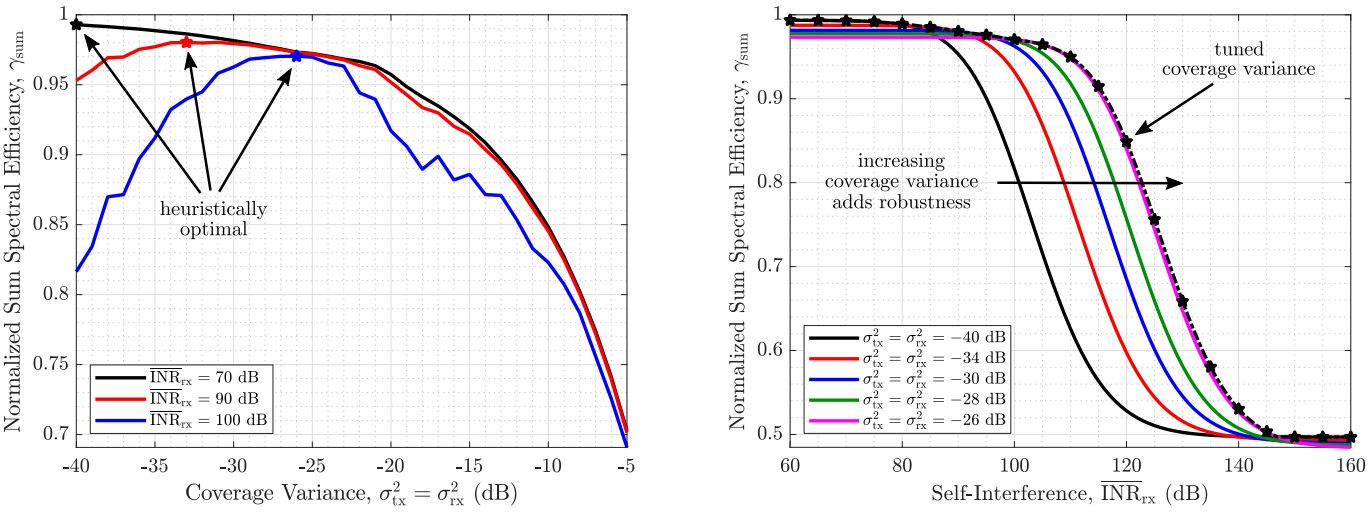

(a) As a function of coverage variance, $\sigma_{\text{tx}}^2 = \sigma_{\text{rx}}^2$.

(b) As a function of self-interference strength, $\overline{\text{INR}}_{\text{rx}}$.

Fig. 6. Normalized sum spectral efficiency γ_{sum} (a) as a function of the coverage variance $\sigma_{\text{tx}}^2 = \sigma_{\text{rx}}^2$ for various $\overline{\text{INR}}_{\text{rx}}$; and (b) as a function of self-interference strength $\overline{\text{INR}}_{\text{rx}}$ for various $\sigma_{\text{tx}}^2 = \sigma_{\text{rx}}^2$. In both, $\overline{\text{SNR}}_{\text{tx}} = \overline{\text{SNR}}_{\text{rx}} = 10$ dB, $b_{\text{phs}} = b_{\text{amp}} = 8$ bits, $\text{INR}_{\text{tx}} = -\infty$ dB, and $\epsilon^2 = -\infty$ dB. Performance with the optimal $\sigma_{\text{tx}}^2 = \sigma_{\text{rx}}^2$ is denoted with $\star$.

near best-case full-duplex performance one can expect when using beamforming codebooks. Having simulated our system in a Monte Carlo fashion, in our results we will present γ_{sum} averaged over downlink-uplink user realizations.

B. Beam Patterns

In Fig. 5, we compare conventional beams to those produced by LoneSTAR. Fig. 5a depicts the shape of beams from our two baseline codebooks. CBF beams can each deliver maximum gain in their steered direction and exhibit a narrow main lobe and high side lobes. With the Taylor codebook, these side lobes are reduced to 25 dB below the main lobe, which itself sacrificed about 6 dB in maximum gain for this side lobe suppression. In Fig. 5b, we plot transmit beams from a codebook produced by LoneSTAR; receive beams are similar. Clearly, unlike the Taylor codebook, LoneSTAR does not attempt to merely shrink side lobes to reduce self-interference. Instead, **LoneSTAR makes use of side lobes, shaping them to cancel self-interference spatially**, and while doing so, maintains near maximum gain across its beams.

C. Choosing Coverage Variances, σ_{tx}^2 and σ_{rx}^2

In general, it is not possible to analytically state optimal choices for the LoneSTAR design parameters σ_{tx}^2 and σ_{rx}^2 which maximize normalized sum spectral efficiency γ_{sum}. This motivates us to examine heuristically how to choose σ_{tx}^2 and σ_{rx}^2. In Fig. 6a, we plot the normalized sum spectral efficiency γ_{sum} as a function of $\sigma_{\text{tx}}^2 = \sigma_{\text{rx}}^2$ for various levels of self-interference $\overline{\text{INR}}_{\text{rx}}$. Here, we let $\overline{\text{SNR}}_{\text{tx}} = \overline{\text{SNR}}_{\text{rx}} = 10$ dB and have assumed no channel estimation error nor cross-link interference (i.e., $\epsilon^2 = -\infty$ dB, $\text{INR}_{\text{tx}} = -\infty$ dB). At low self-interference $\overline{\text{INR}}_{\text{rx}}$ (in black), there is inherently low coupling between the transmit and receive beams, meaning it is best to maintain high beamforming gain rather than reduce self-interference further. This makes a low coverage variance optimal on average, shown as the $\star$ at $\sigma_{\text{tx}}^2 = \sigma_{\text{rx}}^2 = -40$ dB. As $\overline{\text{INR}}_{\text{rx}}$ increases, LoneSTAR benefits from having

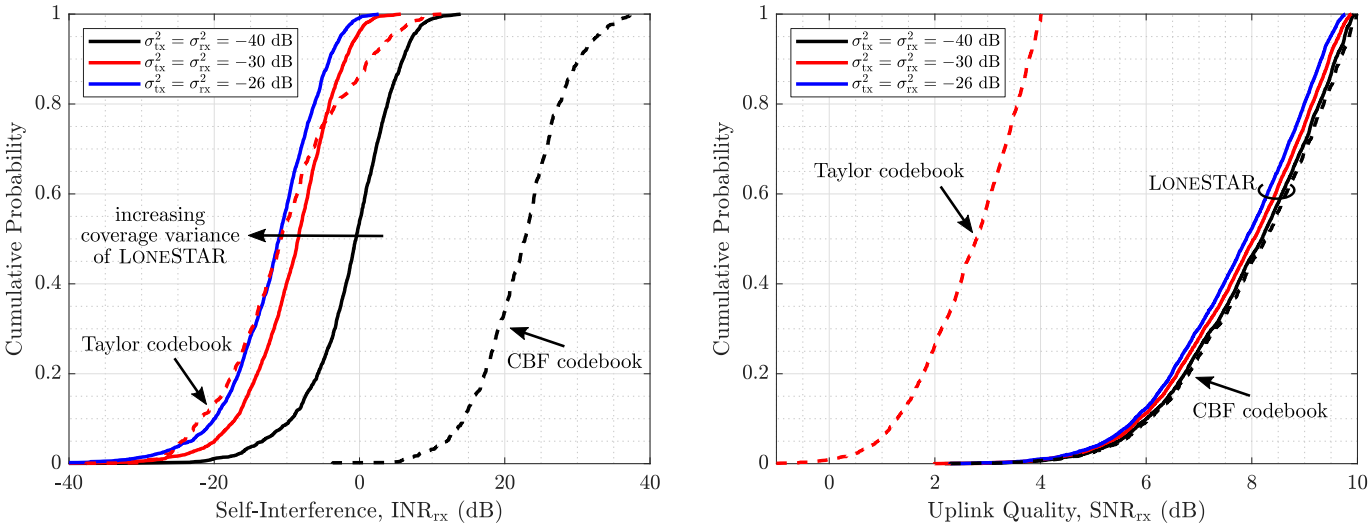

(a) CDF of self-interference, INR_{rx}.

(b) CDF of uplink quality, SNR_{rx}.

Fig. 7. The CDFs of (a) self-interference INR_{rx} where $\overline{\text{INR}}_{\text{rx}} = 90$ dB; and (b) uplink quality SNR_{rx} where $\overline{\text{SNR}}_{\text{rx}} = 10$ dB. LONESTAR ($b_{\text{phs}} = b_{\text{amp}} = 6$ bits) can reduce self-interference between all beam pairs while also maintaining high uplink quality, netting it greater full-duplex performance than conventional codebooks (8 bits).

greater transmit and receive coverage variance since it affords more flexibility to reduce self-interference and increase the sum spectral efficiency.

In Fig. 6b, we highlight this further by plotting the normalized sum spectral efficiency as a function of $\overline{\text{INR}}_{\text{rx}}$ for various $\sigma^2_{\text{tx}} = \sigma^2_{\text{rx}}$. Naturally, one may independently choose σ^2_{tx} and σ^2_{rx}, rather than assume them equal as we have done here for simplicity; this can therefore be considered a conservative evaluation of LONESTAR. The starred curve represents tuning $\sigma^2_{\text{tx}} = \sigma^2_{\text{rx}}$ to maximize sum spectral efficiency at each $\overline{\text{INR}}_{\text{rx}}$. At very low $\overline{\text{INR}}_{\text{rx}}$, full-duplex operation "is free", as transmit and receive beams couple sufficiently low self-interference on their own. In this region, minimizing the coverage variance $\sigma^2_{\text{tx}} = \sigma^2_{\text{rx}}$ is ideal since it preserves near-maximum SNR_{tx} and SNR_{rx}. As $\overline{\text{INR}}_{\text{rx}}$ increases, **increasing $\sigma^2_{\text{tx}} = \sigma^2_{\text{rx}}$ supplies the system with greater robustness to self-interference**, evidenced by the rightward shift of the curves. When $\overline{\text{INR}}_{\text{rx}}$ is overwhelmingly high, LONESTAR cannot mitigate self-interference enough, succumbing to self-interference and offering at most around $\gamma_{\text{sum}} = 0.5$ (essentially half-duplexing). Notice that in this region, it is optimal to return to using very low $\sigma^2_{\text{tx}} = \sigma^2_{\text{rx}}$ in order to preserve half-duplex performance at worst by maximizing SNR. Clearly, choosing $\sigma^2_{\text{tx}} = \sigma^2_{\text{rx}}$ is an important design decision and depends heavily on system factors (chiefly $\overline{\text{INR}}_{\text{rx}}$). In practice, we imagine a system relying on a lookup table to retrieve the optimal σ^2_{tx} and σ^2_{rx} based on its measured $\overline{\text{INR}}_{\text{rx}}$ (along with other system factors), which would likely depend on simulation and experimentation. Henceforth, we assume that the optimal $\sigma^2_{\text{tx}} = \sigma^2_{\text{rx}}$ is used which maximizes γ_{sum}.

VII. COMPARING LONESTAR AGAINST CONVENTIONAL BEAMFORMING CODEBOOKS

Having presented the simulation setup and performance metrics in the previous section, we now compare performance with LONESTAR versus that with conventional codebooks. Consider Fig. 7a, which depicts the cumulative density function (CDF) of INR_{rx} across all transmit-receive beam pairs within LONESTAR codebooks (with $b_{\text{phs}} = b_{\text{amp}} = 6$ bits) versus conventional ones (with 8 bits), where $\overline{\text{INR}}_{\text{rx}} = 90$ dB[3]. For most beam pairs within the CBF codebook, self-interference is typically prohibitively high for full-duplex operation, having $\text{INR}_{\text{rx}} \geq 10$ dB. Very few beam pairs yield $\text{INR}_{\text{rx}} \leq 0$ dB. Desirably, the Taylor codebook can reduce INR_{rx} to well below 0 dB for most beam pairs. Likewise, by increasing the coverage variance $\sigma^2_{\text{tx}} = \sigma^2_{\text{rx}}$, LONESTAR can reduce self-interference between its beam pairs to levels comparable to the Taylor codebook. Note that the difference between LONESTAR and the CBF codebook can be thought of as the amount of self-interference cancellation achieved by LONESTAR.

Now, consider Fig. 7b, which shows the CDF of the resulting uplink quality SNR_{rx} across users, where $\overline{\text{SNR}}_{\text{rx}} = 10$ dB is its upper bound. The CBF codebook can deliver high gain broadly across users, with only a small fraction not within coverage. The Taylor codebook, on the other hand, delivers poor coverage since it sacrificed main lobe gain to shrink its side lobes. For the same three $\sigma^2_{\text{tx}} = \sigma^2_{\text{rx}}$ considered in Fig. 7a, LONESTAR can provide coverage comparable to the CBF codebook, falling short by only about 0.5 dB in distribution. Together, the two evaluations in Fig. 7 highlight how **LONESTAR is capable of offering increased SINR over conventional codebooks by making small sacrifices in coverage to significantly reduce self-interference.**

In Fig. 8, we further compare LONESTAR codebooks against our two baseline codebooks in terms of sum spectral efficiency. We assume no cross-link interference ($\text{INR}_{\text{tx}} =$

[3]We commonly use $\overline{\text{INR}}_{\text{rx}} = 90$ dB since this produces a median INR_{rx} with the CBF codebook that aligns with our INR measurements using an actual 28 GHz phased array platform in [9].

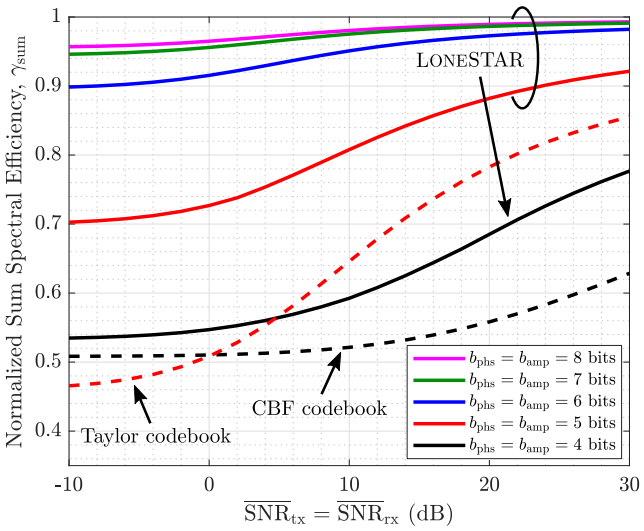

(a) As a function of link quality, $\overline{\text{SNR}}_{\text{tx}} = \overline{\text{SNR}}_{\text{rx}}$.

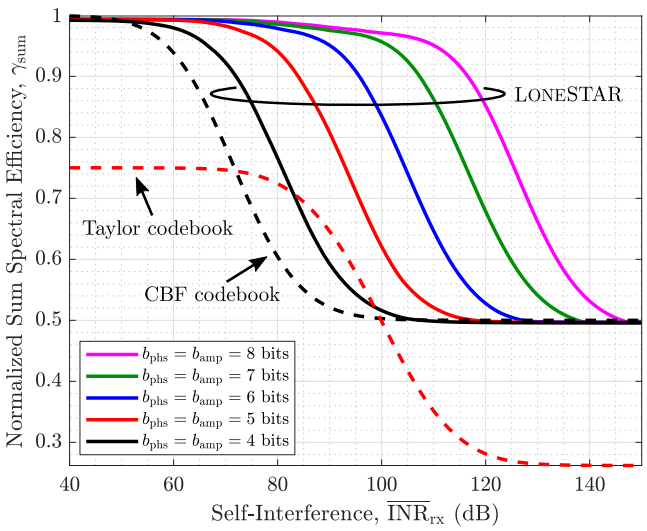

(b) As a function of self-interference strength, $\overline{\text{INR}}_{\text{rx}}$.

Fig. 8. Normalized sum spectral efficiency γ_{sum} (a) as a function of $\overline{\text{SNR}}_{\text{tx}} = \overline{\text{SNR}}_{\text{rx}}$ where $\overline{\text{INR}}_{\text{rx}} = 90$ dB; (b) as a function of $\overline{\text{INR}}_{\text{rx}}$ where $\overline{\text{SNR}}_{\text{tx}} = \overline{\text{SNR}}_{\text{rx}} = 10$ dB. In both, $\text{INR}_{\text{tx}} = -\infty$ dB, $\epsilon^2 = -\infty$ dB, and $\sigma_{\text{tx}}^2 = \sigma_{\text{rx}}^2$ are tuned to maximize sum spectral efficiency. CBF and Taylor codebooks are each with $b_{\text{phs}} = b_{\text{amp}} = 8$ bits.

$-\infty$ dB) and no channel estimation error ($\epsilon^2 = -\infty$ dB); we will evaluate LoneSTAR against both of these shortly. In Fig. 8a, we plot the normalized sum spectral efficiency γ_{sum} achieved by LoneSTAR as a function of $\overline{\text{SNR}}_{\text{tx}} = \overline{\text{SNR}}_{\text{rx}}$ for various resolutions $b_{\text{phs}} = b_{\text{amp}}$, where $\overline{\text{INR}}_{\text{rx}} = 90$ dB. The CBF and Taylor codebooks were both configured with $b_{\text{phs}} = b_{\text{amp}} = 8$ bits. At low $\overline{\text{SNR}}_{\text{tx}} = \overline{\text{SNR}}_{\text{rx}}$, the CBF codebook can deliver $\gamma_{\text{sum}} \approx 0.5$, since the receive link is overwhelmed by self-interference while the transmit link sees nearly full beamforming gain. The Taylor codebook sacrifices beamforming gain to reduce its side lobes and therefore achieves only $\gamma_{\text{sum}} \approx 0.46$ at low $\overline{\text{SNR}}_{\text{tx}} = \overline{\text{SNR}}_{\text{rx}}$. As $\overline{\text{SNR}}_{\text{tx}} = \overline{\text{SNR}}_{\text{rx}}$ increases, CBF and Taylor codebooks naturally both improve their performance as the impacts of self-interference diminish with increased SNR. Shown as solid lines, LoneSTAR improves significantly as $b_{\text{phs}} = b_{\text{amp}}$ increases from 4 bits to 8 bits. Even at low $\overline{\text{SNR}}_{\text{tx}} = \overline{\text{SNR}}_{\text{rx}}$, **LoneSTAR can deliver sum spectral efficiencies well above that of conventional codebooks by better rejecting self-interference while maintaining high beamforming gain.** This is especially true when $b_{\text{phs}} = b_{\text{amp}} \geq 6$ bits, which allows LoneSTAR to deliver upwards of 90% of the full-duplex codebook capacity. At high SNR, LoneSTAR naturally improves, saturating due to diminishing gains in $\log_2(1+x)$. For $\overline{\text{SNR}}_{\text{tx}} = \overline{\text{SNR}}_{\text{rx}} \geq 5$ dB, the Taylor codebook can significantly outperform the CBF codebook and can marginally outperform LoneSTAR having $b_{\text{phs}} = b_{\text{amp}} = 4$ bits, especially at high SNR.

In Fig. 8b, we now fix $\overline{\text{SNR}}_{\text{tx}} = \overline{\text{SNR}}_{\text{rx}} = 10$ dB and vary $\overline{\text{INR}}_{\text{rx}}$, keeping all other factors the same as in Fig. 8a. CBF and LoneSTAR both can nearly reach the full-duplex codebook capacity at low $\overline{\text{INR}}_{\text{rx}}$, where self-interference is negligible and near maximal beamforming gain can be delivered. The Taylor codebook sacrifices beamforming gain for reduced side lobes and therefore falls well short of $\gamma_{\text{sum}} = 1$, even in the presence of extremely weak self-interference. **As $\overline{\text{INR}}_{\text{rx}}$ is increased, CBF quickly succumbs to self-interference, whereas LoneSTAR proves to be notably more robust to such.** In fact, with each unit increase in resolution $b_{\text{phs}} = b_{\text{amp}}$, LoneSTAR supplies around 10 dB of added robustness to self-interference. The Taylor codebook can outperform the CBF codebook but only for $\overline{\text{INR}}_{\text{rx}} \in [72, 100]$ dB before also being overwhelmed by self-interference. At higher SNR, when $\overline{\text{SNR}}_{\text{tx}} = \overline{\text{SNR}}_{\text{rx}} \geq 10$ dB, this $\overline{\text{INR}}_{\text{rx}}$ range would widen, as evidenced by Fig. 8a. As $\overline{\text{INR}}_{\text{rx}}$ increases to extremely high levels, LoneSTAR converges to offer nearly the same sum spectral efficiency as CBF of $\gamma_{\text{sum}} = 0.5$, essentially only serving the downlink user due to uplink being overwhelmed by self-interference. Each full-duplex mmWave BS will see a unique $\overline{\text{INR}}_{\text{rx}}$ depending on a variety of parameters including transmit power, noise power, and isolation between its transmit and receive arrays. This makes LoneSTAR an attractive codebook design since it is more robust than conventional codebooks over a wide range of $\overline{\text{INR}}_{\text{rx}}$ and provides greater flexibility when designing full-duplex mmWave platforms. With LoneSTAR, systems can operate at higher $\overline{\text{INR}}_{\text{rx}}$, meaning they can potentially increase transmit power without being severely penalized by increased self-interference, for instance.

A. For Various Link Qualities, $\left(\overline{\text{SNR}}_{\text{tx}}, \overline{\text{SNR}}_{\text{rx}}\right)$

Rather than assume symmetric downlink/uplink quality $\overline{\text{SNR}}_{\text{tx}} = \overline{\text{SNR}}_{\text{rx}}$, we now consider $\overline{\text{SNR}}_{\text{tx}} \neq \overline{\text{SNR}}_{\text{rx}}$. In Fig. 9a, we show the normalized sum spectral efficiency achieved by the Taylor codebook as a function of $\left(\overline{\text{SNR}}_{\text{tx}}, \overline{\text{SNR}}_{\text{rx}}\right)$, where $\overline{\text{INR}}_{\text{rx}} = 90$ dB and $b_{\text{phs}} = b_{\text{amp}} = 8$ bits. In Fig. 9b, we show that of LoneSTAR with $b_{\text{phs}} = b_{\text{amp}} = 6$ bits. We chose to compare against the Taylor codebook rather than the CBF codebook because it better competes

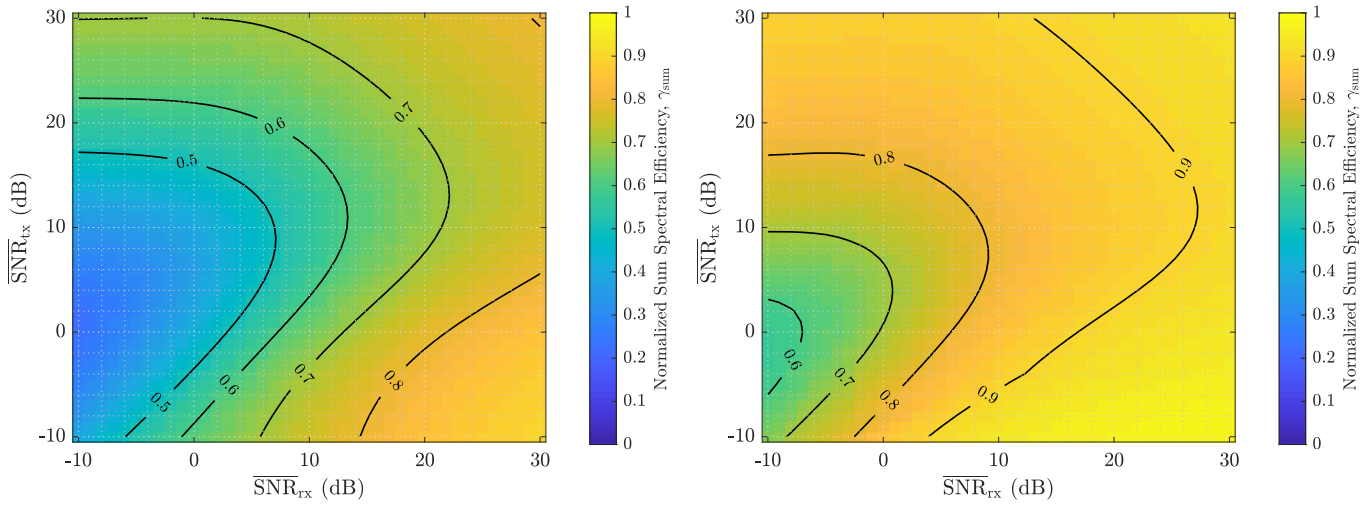

(a) Taylor codebook. (b) LONESTAR codebooks.

Fig. 9. Normalized sum spectral efficiency γ_{sum} as a function of $\left(\overline{\mathsf{SNR}}_{\mathrm{tx}}, \overline{\mathsf{SNR}}_{\mathrm{rx}}\right)$ for the (a) Taylor codebook ($b_{\mathrm{phs}} = b_{\mathrm{amp}} = 8$ bits) and (b) LONESTAR codebooks, where $\overline{\mathsf{INR}}_{\mathrm{rx}} = 90$ dB, $\mathsf{INR}_{\mathrm{tx}} = -\infty$ dB, $b_{\mathrm{phs}} = b_{\mathrm{amp}} = 6$ bits, and $\epsilon^2 = -\infty$ dB. LONESTAR delivers higher γ_{sum} broadly across SNRs and demands lower SNRs to net $\gamma_{\mathrm{sum}} \geq 0.5$.

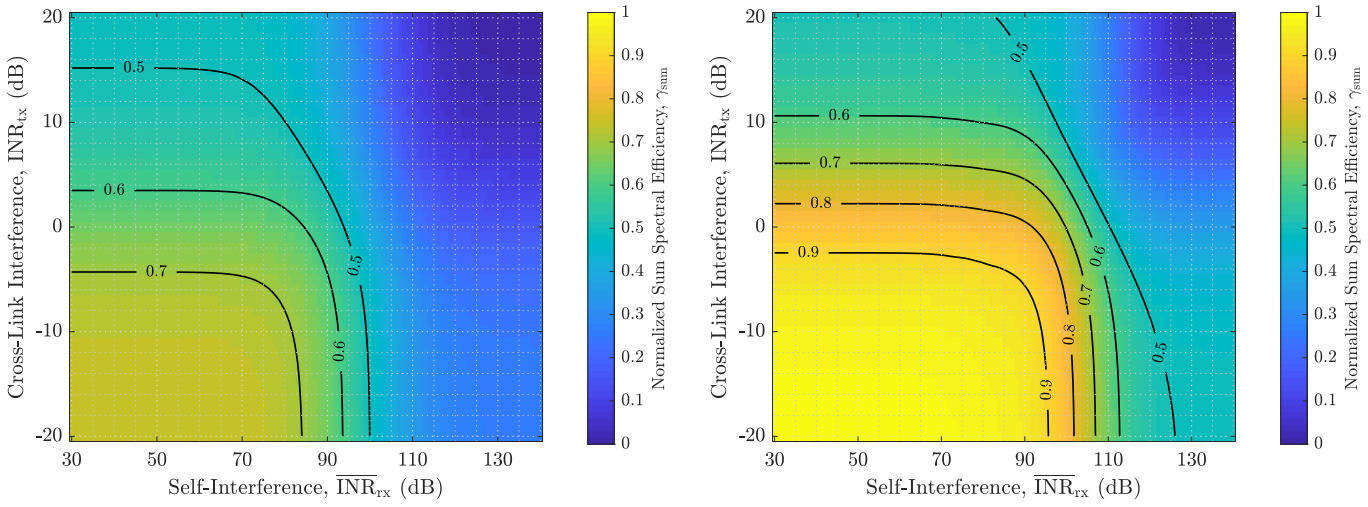

(a) Taylor codebook. (b) LONESTAR codebooks.

Fig. 10. Normalized sum spectral efficiency γ_{sum} as a function of $\left(\mathsf{INR}_{\mathrm{tx}}, \overline{\mathsf{INR}}_{\mathrm{rx}}\right)$ for the (a) Taylor codebook, where $b_{\mathrm{phs}} = b_{\mathrm{amp}} = 8$ bits; and (b) LONESTAR codebooks, where $b_{\mathrm{phs}} = b_{\mathrm{amp}} = 6$ bits. In both, $\overline{\mathsf{SNR}}_{\mathrm{tx}} = \overline{\mathsf{SNR}}_{\mathrm{rx}} = 10$ dB and $\epsilon^2 = -\infty$ dB. LONESTAR is more robust to self-interference and cross-link interference than conventional codebooks.

with LONESTAR at $\overline{\mathsf{INR}}_{\mathrm{rx}} = 90$ dB (see Fig. 8a). Clearly, **LONESTAR can deliver higher spectral efficiencies than the Taylor codebook broadly over $\left(\overline{\mathsf{SNR}}_{\mathrm{tx}}, \overline{\mathsf{SNR}}_{\mathrm{rx}}\right)$.** It is important to notice that the region where $\gamma_{\mathrm{sum}} \geq 0.5$—where full-duplexing is superior to half-duplexing with equal TDD—grows significantly with LONESTAR versus the Taylor codebook. This means that full-duplex operation is justified over a much broader range of $\left(\overline{\mathsf{SNR}}_{\mathrm{tx}}, \overline{\mathsf{SNR}}_{\mathrm{rx}}\right)$ with LONESTAR compared to with conventional codebooks. It is also important to notice that **LONESTAR introduces a significant SNR gain versus conventional codebooks**, since it demands a much lower $\left(\overline{\mathsf{SNR}}_{\mathrm{tx}}, \overline{\mathsf{SNR}}_{\mathrm{rx}}\right)$ to achieve a desired sum spectral efficiency.Note that we have tuned $\sigma^2_{\mathrm{tx}} = \sigma^2_{\mathrm{rx}}$, meaning the performance of LONESTAR may improve if σ^2_{tx} and σ^2_{rx} were tuned separately, especially with highly asymmetric SNRs.

B. For Various Levels of Interference, $\left(\mathsf{INR}_{\mathrm{tx}}, \overline{\mathsf{INR}}_{\mathrm{rx}}\right)$

Similar to Fig. 9, we now compare the Taylor codebook against LONESTAR for various $\left(\mathsf{INR}_{\mathrm{tx}}, \overline{\mathsf{INR}}_{\mathrm{rx}}\right)$ in Fig. 10, where we have fixed $\overline{\mathsf{SNR}}_{\mathrm{tx}} = \overline{\mathsf{SNR}}_{\mathrm{rx}} = 10$ dB. Again, LONESTAR can clearly deliver much higher spectral efficiencies than the Taylor codebook, achieving nearly the full-duplex codebook capacity when cross-link interference and self-interference are both low. Even at very low INRs, the Taylor codebook cannot approach $\gamma_{\mathrm{sum}} = 1$ since it sacrificed beamforming gain for side lobe suppression. At high INRs,

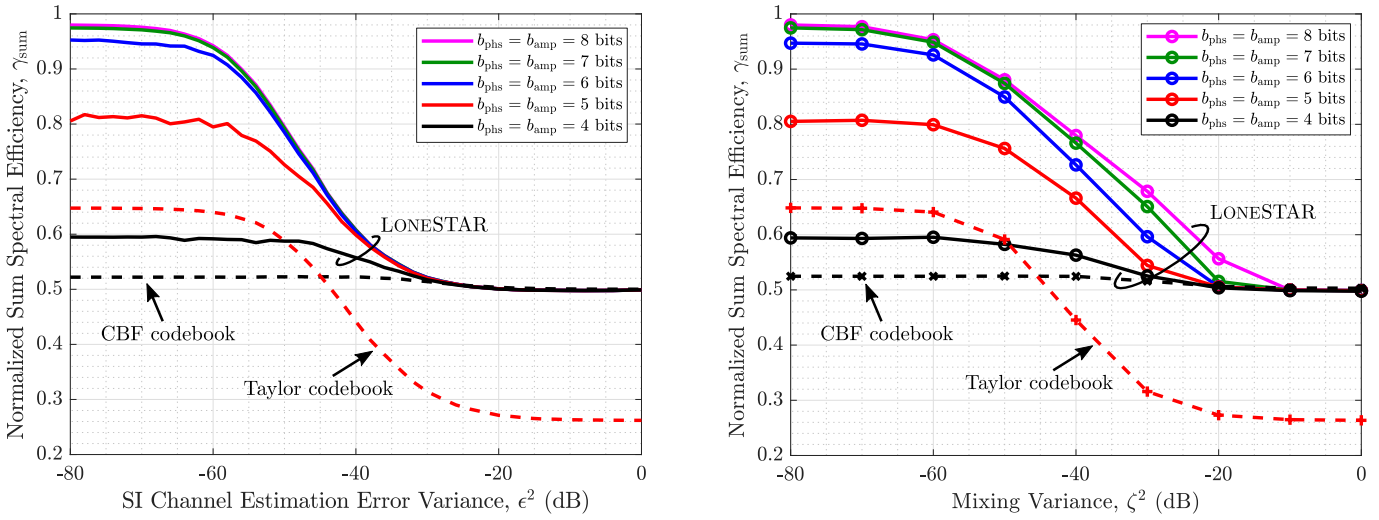

(a) Channel estimation error.

(b) Gaussian mixing.

Fig. 11. Normalized sum spectral efficiency as a function of (a) self-interference channel estimation error variance ϵ^2 and (b) mixing variance ζ^2. In both, $\overline{\mathsf{SNR}}_{\text{tx}} = \overline{\mathsf{SNR}}_{\text{rx}} = 10$ dB, $\overline{\mathsf{INR}}_{\text{rx}} = 90$ dB, and $\mathsf{INR}_{\text{tx}} = -\infty$ dB. The true channel $\mathbf{H}$ is distributed the same in both, but in (b), we assume perfect channel knowledge, $\epsilon^2 = -\infty$ dB.

both LoneSTAR and the Taylor codebook struggle to deliver high γ_{sum}, largely due to the fact that neither can reduce cross-link interference. In between, at moderate INRs, LoneSTAR can sustain spectral efficiencies notably higher than the Taylor codebook. **LoneSTAR's added robustness to cross-link interference and self-interference is on display here**, as it can tolerate higher $\left(\mathsf{INR}_{\text{tx}}, \overline{\mathsf{INR}}_{\text{rx}}\right)$ than the Taylor codebook while delivering the same γ_{sum}. This is thanks to LoneSTAR's ability to net a higher receive link spectral efficiency, which can yield a higher sum spectral efficiency in the presence of high cross-link interference INR_{tx}. At an $\overline{\mathsf{INR}}_{\text{rx}} = 50$ dB, for example, LoneSTAR provides around 10 dB of robustness to INR_{tx} for $\gamma_{\text{sum}} = 0.7$, compared to the Taylor codebook. At an $\mathsf{INR}_{\text{tx}} = -10$ dB, LoneSTAR provides around 30 dB of robustness to self-interference $\overline{\mathsf{INR}}_{\text{rx}}$ for $\gamma_{\text{sum}} = 0.7$.

C. Impact of Channel Estimation Error and Channel Structure

Now, in Fig. 11a, we examine the impacts of imperfect self-interference channel knowledge, $\epsilon^2 > -\infty$ dB. To do so, we model $\bar{\mathbf{H}}$ as in (45), meaning the true channel $\mathbf{H}$ is Gaussian distributed about $\bar{\mathbf{H}}$ according to (12). We chose to model it in this fashion, rather than use $\mathbf{H}$ as the spherical-wave model in (45), for two reasons. First, it is more challenging for LoneSTAR to face a channel under this mixed model (as we will see shortly in Fig. 11b). Second, it represents the potential case where the estimate $\bar{\mathbf{H}}$ is computed directly based on the relative geometry of the transmit and receive arrays using the spherical-wave model (which can be done *a priori*) and the estimation error captures deviations from this assumed spherical-wave behavior. In Fig. 11a, we plot the normalized sum spectral efficiency as a function of self-interference channel estimation error variance ϵ^2. With accurate estimation of $\mathbf{H}$, LoneSTAR performs quite well as it has proven thus far. As the quality of estimation degrades, LoneSTAR has difficulty reliably avoiding self-interference. Its performance suffers but remains well above $\gamma_{\text{sum}} = 0.5$ before converging to performance offered by the CBF codebook around $\epsilon^2 = -30$ dB. The CBF codebook sees mild degradation with increased estimation error. Clearly, the Taylor codebook, like LoneSTAR, suffers as ϵ^2 increases. It may seem strange that the CBF and Taylor codebooks both vary as a function of estimation error ϵ^2 since neither codebook depends on self-interference channel knowledge. This can be explained by the fact that the estimation error $\mathbf{\Delta}$ is distributed differently than the estimate $\bar{\mathbf{H}}$. In other words, the Taylor codebook is inherently more robust to the more structured spherical-wave self-interference channel than a Gaussian one. **Gaussian-distributed error proves to be especially difficult for LoneSTAR and Taylor to endure.** As such, it is evident that imperfect channel knowledge *and* the fact that estimation error is Gaussian both contribute to LoneSTAR's degradation as ϵ^2 increases.

We dissect the impacts of estimation error versus that of mixing the spherical-wave model with a Gaussian matrix in Fig. 11b by considering the mixed self-interference channel model

$$\mathbf{H} = \frac{\mathbf{H}_{\text{SW}} + \mathbf{H}_{\text{Ray}}}{\|\mathbf{H}_{\text{SW}} + \mathbf{H}_{\text{Ray}}\|_{\text{F}}} \cdot \sqrt{N_{\text{t}} \cdot N_{\text{r}}}, \tag{50}$$

where $\mathbf{H}_{\text{SW}}$ is the spherical-wave model defined in (45) and $\mathbf{H}_{\text{Ray}}$ is Rayleigh faded with variance ζ^2 defined as

$$[\mathbf{H}_{\text{Ray}}]_{m,n} \sim \mathcal{N}_{\mathbb{C}}\left(0, \zeta^2\right) \ \forall \ m, n. \tag{51}$$

The scaling in (50) simply ensures $\|\mathbf{H}\|_{\text{F}}^2 = N_{\text{t}} \cdot N_{\text{r}}$. We evaluate LoneSTAR using this channel model for various ζ^2, which we term the *mixing variance*. In doing so, we assume perfect knowledge of the realized channel $\mathbf{H}$ (i.e., $\epsilon^2 = -\infty$ dB) to solely investigate the effects of this mixing. The spherical-wave channel $\mathbf{H}_{\text{SW}}$ is a highly structured channel based on the relative geometry between the transmit and

receive arrays at the BS. The Rayleigh faded channel $\mathbf{H}_{\text{Ray}}$ (a Gaussian matrix) lay at the other extreme, lacking any inherent structure. It is important to notice that the distribution of true channel $\mathbf{H}$ here is identical to that examined in Fig. 11a. In this case, however, we consider $\epsilon^2 = -\infty$ dB to investigate the impacts of $\mathbf{H}$ becoming increasingly Gaussian, rather than those stemming from imperfect channel knowledge.

In Fig. 11b, we plot the normalized sum spectral efficiency as a function of the mixing variance ζ^2. Having considered perfect channel knowledge $\epsilon^2 = -\infty$ dB here, Fig. 11b is an upper bound on Fig. 11a since they follow the same channel model. At very low ζ^2, $\mathbf{H} \approx \mathbf{H}_{\text{SW}}$, allowing LONESTAR to achieve appreciable spectral efficiencies above conventional codebooks, as we have seen thus far. As ζ^2 increases, the sum spectral efficiency offered by LONESTAR tends to decrease, though so does the Taylor codebook and the CBF codebook slightly so. At high ζ^2, LONESTAR suffers since it cannot find ways to pack the transmit and receive beams such that they do not couple across the self-interference channel. This is intimately related to the fact that Gaussian matrices (almost surely) tend to inflict self-interference across all dimensions of $\mathbf{H}$, making it a statistically more difficult channel for LONESTAR to build codebooks that minimize transmit-receive beam coupling. **Thus, even with perfect channel estimation, LONESTAR struggles with self-interference channels that are too heavily Gaussian.** However, with modest Gaussian mixing (e.g., $\zeta^2 = -40$ dB), LONESTAR can deliver appreciable spectral efficiency with accurate channel estimation. From the results in Fig. 11, we observe that there is the need for accurate and perhaps frequent self-interference channel estimation. Our hope is that this can be accomplished by taking advantage of the strength of the self-interference channel, along with a potentially known channel structure (e.g., [34]) and occasional—but thorough—measurements at the BS, as mentioned in Section III. To overcome challenges associated with Gaussian channels, future work may extend LONESTAR to the design of a single higher-dimensional codebook of transmit-receive beam pairs $(\mathbf{f}, \mathbf{w})$ that are jointly selected following beam alignment (e.g., similar to [24]).

VIII. CONCLUSION AND FUTURE DIRECTIONS

Conventional beamforming codebooks are not suitable for full-duplex mmWave systems since they do not offer much robustness to self-interference. Meanwhile, existing beamforming-based solutions for full-duplex mmWave systems typically do not support codebook-based beam alignment, demand real-time knowledge of high-dimensional downlink/uplink MIMO channels, and do not scale well when serving many users over time—all of which are practical shortcomings. We have presented LONESTAR, a novel approach to enable full-duplex mmWave communication systems through the design of analog beamforming codebooks that are robust to self-interference. Our design does not rely on downlink/uplink channel knowledge and therefore need only be executed once per coherence time of the self-interference channel, allowing the same LONESTAR codebooks to be used for beam alignment and to serve many downlink-uplink user pairs thereafter. We illustrated that LONESTAR can mitigate self-interference to levels sufficiently low for appreciable spectral efficiency gains compared to conventional codebooks by being more robust to self-interference and cross-link interference broadly across downlink and uplink SNRs.

This work has motivated a variety of future work for full-duplex mmWave systems. Extensive study and modeling of mmWave self-interference channels and their coherence time will be important to understanding the potentials of LONESTAR—and full-duplex mmWave systems in general—along with developing efficient means for self-interference channel estimation. Also, methods to dynamically update LONESTAR as the self-interference channel drifts would be valuable future work, along with implementations of LONESTAR using real mmWave platforms. Naturally, there are other ways to improve upon this work, such as by better handling limited phase and amplitude control and by creating efficient, dedicated solvers for LONESTAR. Beyond LONESTAR, measurement-driven beamforming-based full-duplex solutions (potentially using machine learning) that do not require self-interference MIMO channel knowledge (e.g., STEER [24]) would be excellent contributions to the research community.

ACKNOWLEDGMENTS

We thank Marius Arvinte and Ruichen Jiang for their discussions and insights related to our design formulation.

REFERENCES

[1] I. P. Roberts, H. B. Jain, S. Vishwanath, and J. G. Andrews, "Millimeter wave analog beamforming codebooks robust to self-interference," in *Proc. IEEE GLOBECOM*, Dec. 2021, pp. 1–6.

[2] R. W. Heath, N. González-Prelcic, S. Rangan, W. Roh, and A. M. Sayeed, "An overview of signal processing techniques for millimeter wave MIMO systems," *IEEE J. Sel. Topics Signal Process.*, vol. 10, no. 3, pp. 436–453, Apr. 2016.

[3] Y. Heng *et al.*, "Six key challenges for beam management in 5.5G and 6G systems," *IEEE Commun. Mag.*, vol. 59, no. 7, pp. 74–79, Jul. 2021.

[4] J. Wang *et al.*, "Beam codebook based beamforming protocol for multi-Gbps millimeter-wave WPAN systems," *IEEE J. Sel. Areas Commun.*, vol. 27, no. 8, pp. 1390–1399, Oct. 2009.

[5] R. W. Heath Jr. and A. Lozano, *Foundations of MIMO Communication*. Cambridge: Cambridge University Press, 2018.

[6] R. J. Mailloux, *Phased Array Antenna Handbook*. Norwood, MA, USA: Artech House, 2005.

[7] T. Taylor, "Design of line-source antennas for narrow beamwidth and low side lobes," *Transactions of the IRE Professional Group on Antennas and Propagation*, vol. 3, no. 1, pp. 16–28, Jan. 1955.

[8] W. G. Carrara, R. S. Goodman, and R. M. Majewski, *Spotlight Synthetic Aperture Radar: Signal Processing Algorithms*. Norwood, MA, USA: Artech House, 1995.

[9] I. P. Roberts, A. Chopra, T. Novlan, S. Vishwanath, and J. G. Andrews, "Beamformed self-interference measurements at 28 GHz: Spatial insights and angular spread," *IEEE Trans. Wireless Commun.*, vol. 21, no. 11, pp. 9744–9760, Nov. 2022.

[10] I. P. Roberts, J. G. Andrews, H. B. Jain, and S. Vishwanath, "Millimeter-wave full duplex radios: New challenges and techniques," *IEEE Wireless Commun.*, vol. 28, no. 1, pp. 36–43, Feb. 2021.

[11] A. Sabharwal *et al.*, "In-band full-duplex wireless: Challenges and opportunities," *IEEE J. Sel. Areas Commun.*, vol. 32, no. 9, pp. 1637–1652, Sep. 2014.

[12] K. Satyanarayana, M. El-Hajjar, P. Kuo, A. Mourad, and L. Hanzo, "Hybrid beamforming design for full-duplex millimeter wave communication," *IEEE Trans. Veh. Technol.*, vol. 68, no. 2, pp. 1394–1404, Feb. 2019.

[13] X. Liu *et al.*, "Beamforming based full-duplex for millimeter-wave communication," *Sensors*, vol. 16, no. 7, p. 1130, Jul. 2016.

[14] R. López-Valcarce and N. González-Prelcic, "Analog beamforming for full-duplex millimeter wave communication," in *Proc. ISWCS*, Aug. 2019, pp. 687–691.
[15] ——, "Beamformer design for full-duplex amplify-and-forward millimeter wave relays," in *Proc. ISWCS*, Aug. 2019, pp. 86–90.
[16] J. Palacios, J. Rodríguez-Fernández, and N. González-Prelcic, "Hybrid precoding and combining for full-duplex millimeter wave communication," in *Proc. IEEE GLOBECOM*, Dec. 2019, pp. 1–6.
[17] L. Zhu *et al.*, "Millimeter-wave full-duplex UAV relay: Joint positioning, beamforming, and power control," *IEEE J. Sel. Areas Commun.*, vol. 38, no. 9, pp. 2057–2073, Sep. 2020.
[18] Y. Cai, Y. Xu, Q. Shi, B. Champagne, and L. Hanzo, "Robust joint hybrid transceiver design for millimeter wave full-duplex MIMO relay systems," *IEEE Trans. Wireless Commun.*, vol. 18, no. 2, pp. 1199–1215, Feb. 2019.
[19] A. Koc and T. Le-Ngoc, "Full-duplex mmWave massive MIMO systems: A joint hybrid precoding/combining and self-interference cancellation design," *IEEE Open J. Commun. Society*, vol. 2, pp. 754–774, Mar. 2021.
[20] R. López-Valcarce and M. Martínez-Cotelo, "Full-duplex mmWave MIMO with finite-resolution phase shifters," *IEEE Trans. Wireless Commun.*, May 2022, (early access).
[21] J. M. B. da Silva, A. Sabharwal, G. Fodor, and C. Fischione, "1-bit phase shifters for large-antenna full-duplex mmWave communications," *IEEE Trans. Wireless Commun.*, vol. 19, no. 10, pp. 6916–6931, Oct. 2020.
[22] I. P. Roberts, J. G. Andrews, and S. Vishwanath, "Hybrid beamforming for millimeter wave full-duplex under limited receive dynamic range," *IEEE Trans. Wireless Commun.*, vol. 20, no. 12, pp. 7758–7772, Dec. 2021.
[23] S. Huberman and T. Le-Ngoc, "MIMO full-duplex precoding: A joint beamforming and self-interference cancellation structure," *IEEE Trans. Wireless Commun.*, vol. 14, no. 4, pp. 2205–2217, Apr. 2015.
[24] I. P. Roberts, A. Chopra, T. Novlan, S. Vishwanath, and J. G. Andrews, "STEER: Beam selection for full-duplex millimeter wave communication systems," *IEEE Trans. Commun.*, vol. 70, no. 10, pp. 6902–6917, Oct. 2022.
[25] A. Natarajan *et al.*, "A fully-integrated 16-element phased-array receiver in SiGe BiCMOS for 60-GHz communications," *IEEE J. Solid-State Circuits*, vol. 46, no. 5, pp. 1059–1075, May 2011.
[26] B. Sadhu *et al.*, "A 28-GHz 32-element TRX phased-array IC with concurrent dual-polarized operation and orthogonal phase and gain control for 5G communications," *IEEE J. Solid-State Circuits*, vol. 52, no. 12, pp. 3373–3391, Dec. 2017.
[27] "5G Products | Anokiwave," 2021. [Online]. Available: https://www.anokiwave.com/5g/index.html
[28] C. Dehos, J. L. González, A. D. Domenico, D. Kténas, and L. Dussopt, "Millimeter-wave access and backhauling: the solution to the exponential data traffic increase in 5G mobile communications systems?" *IEEE Commun. Mag.*, vol. 52, no. 9, pp. 88–95, Sep. 2014.
[29] 3GPP, "TS 38.174: New WID on IAB enhancements." [Online]. Available: https://www.3gpp.org/dynareport/38174.htm
[30] M. Gupta, I. P. Roberts, and J. G. Andrews, "System-level analysis of full-duplex self-backhauled millimeter wave networks," *IEEE Trans. Wireless Commun.*, Sep. 2022, (early access).
[31] G. Y. Suk *et al.*, "Full duplex integrated access and backhaul for 5G NR: Analyses and prototype measurements," *IEEE Wireless Commun.*, May 2022, (early access).
[32] Z. Wei *et al.*, "Full-duplex versus half-duplex amplify-and-forward relaying: Which is more energy efficient in 60-GHz dual-hop indoor wireless systems?" vol. 33, no. 12, pp. 2936–2947, Dec. 2015.
[33] C. Balanis, *Antenna Theory: Analysis and Design*. Hoboken, New Jersey: John Wiley & Sons, 2016.
[34] M. Cui and L. Dai, "Channel estimation for extremely large-scale MIMO: Far-field or near-field?" *IEEE Trans. Wireless Commun.*, vol. 70, no. 4, pp. 2663–2677, Apr. 2022.
[35] S. Boyd and L. Vandenberghe, *Convex Optimization*. Cambridge: Cambridge University Press, 2004.
[36] A. B. Gershman, N. D. Sidiropoulos, S. Shahbazpanahi, M. Bengtsson, and B. Ottersten, "Convex optimization-based beamforming," *IEEE Signal Process. Mag.*, vol. 27, no. 3, pp. 62–75, May 2010.
[37] X. Zhang, D. P. Palomar, and B. Ottersten, "Statistically robust design of linear MIMO transceivers," *IEEE Trans. Signal Process.*, vol. 56, no. 8, pp. 3678–3689, Aug. 2008.
[38] J. Wang and D. P. Palomar, "Worst-case robust MIMO transmission with imperfect channel knowledge," *IEEE Trans. Signal Process.*, vol. 57, no. 8, pp. 3086–3100, Aug. 2009.
[39] A. K. Gupta and D. K. Nagar, *Matrix Variate Distributions*. Boca Raton, FL, USA: Chapman & Hall/CRC, 2000.
[40] M. Grant and S. Boyd, "CVX: Software for disciplined convex programming, version 2.1," http://cvxr.com/cvx, Mar. 2014.
[41] I. P. Roberts, "MIMO for MATLAB: A toolbox for simulating MIMO communication systems," Nov. 2021. [Online]. Available: https://arxiv.org/abs/2111.05273
[42] J.-S. Jiang and M. A. Ingram, "Spherical-wave model for short-range MIMO," *IEEE Trans. Commun.*, vol. 53, no. 9, pp. 1534–1541, Sep. 2005.

Ian P. Roberts (Graduate Student Member, IEEE) received the B.S. degree in electrical engineering from the Missouri University of Science and Technology and the M.S. degree in electrical and computer engineering from the University of Texas at Austin, where he is currently a Ph.D. candidate and part of 6G@UT in the Wireless Networking and Communications Group. He has industry experience developing and prototyping wireless technologies at AT&T Labs, Amazon, GenXComm (startup), and Sandia National Laboratories. His research interests are in the theory and implementation of millimeter wave systems, in-band full-duplex, and other next-generation technologies for wireless communication and sensing. He is a National Science Foundation Graduate Research Fellow.

Sriram Vishwanath (Fellow, IEEE) received the B.Tech. degree in Electrical Engineering from the Indian Institute of Technology (IIT), Madras, India, in 1998, the M.S. degree in Electrical Engineering from California Institute of Technology (Caltech), Pasadena, CA, USA, in 1999, and the Ph.D. degree in Electrical Engineering from Stanford University, Stanford, CA, USA, in 2003. For the past 18 years, he has been a Professor of Electrical and Computer Engineering at The University of Texas at Austin.

Sriram's research is in the domains of wireless networking and systems, information and coding theory, machine learning systems, and blockchain systems. He has over 300 refereed research papers and multiple research awards. He works across a diverse set of areas and specializes in bridging the gap between theory and practice. In particular, he has been involved in multiple spinouts from The University of Texas (as well as startups independent from The University of Texas).

Sriram received the NSF CAREER award in 2005 and the ARO Young Investigator Award in 2008. He was the UT Faculty Entrepreneur of the Year in 2014. He is a Fellow of the IEEE.

Jeffrey G. Andrews (Fellow, IEEE) received the B.S. in Engineering with High Distinction from Harvey Mudd College, and the M.S. and Ph.D. in Electrical Engineering from Stanford University. He is the Truchard Family Chair in Engineering at the University of Texas at Austin where he is Director of the 6G@UT research center. He developed CDMA systems at Qualcomm, and has served as a consultant to Samsung, Nokia, Qualcomm, Apple, Verizon, AT&T, Intel, Microsoft, Sprint, and NASA. He is co-author of the books *Fundamentals of WiMAX* (Prentice-Hall, 2007) and *Fundamentals of LTE* (Prentice-Hall, 2010). He was the Editor-in-Chief of the IEEE TRANSACTIONS ON WIRELESS COMMUNICATIONS from 2014-2016, and is the founding Chair of the Steering Committee for the IEEE JOURNAL ON SELECTED AREAS IN INFORMATION THEORY (2018-23), and was Chair of the IEEE Communication Theory Technical Committee (2021-22).

Dr. Andrews is an IEEE Fellow and ISI Highly Cited Researcher and has been co-recipient of 16 best paper awards including the 2016 IEEE Communications Society & Information Theory Society Joint Paper Award, the 2014 IEEE Stephen O. Rice Prize, the 2014 and 2018 IEEE Leonard G. Abraham Prize, the 2011 and 2016 IEEE Heinrich Hertz Prize, and the 2010 IEEE ComSoc Best Tutorial Paper Award. His other major awards include the 2015 Terman Award, the NSF CAREER Award, the 2021 Gordon Lepley Memorial Teaching Award at UT Austin, the 2021 IEEE ComSoc Joe LoCicero Service Award, the 2019 IEEE Wireless Communications Technical Committee Recognition Award, and the 2019 IEEE Kiyo Tomiyasu Award, which is an IEEE Technical Field Award.